Studies on the Composition, Distribution and Detection of Dark Matter in the Universe

Dissertation
submitted for the award of the degree of
Master of Philosophy
in
Physics
by

Sajad Hussain Bhat

Under the Supervision of

Dr. Manzoor A. Malik

Department of Physics,
University of Kashmir, Srinagar, 190 006

Acknowledgments

First and foremost, I would like to express my gratitude to my supervisor Dr. Manzoor A. Malik for the opportunity to work on the subject of Dark matter. As a student I have learned to appreciate his profound knowledge of the subject and intuition for the essential as well as his manner of researching and special unique point of views. His concern towards his students makes him a sublime and unique personality in the whole university.

Next, I would like to thank Prof. Javaid Ahmad Sheikh, Head of the Department of Physics for providing me all the support during my research. My special thanks go to Dr. Waseem Bari and Farooq Hussain Bhat(IUST) for their constant guidance and support.

I express my heartfelt thanks to my parents who despite all odds provided the unconditional love and support thorough out my life. I would like to take this opportunity to thank my loving sister, Without her support I would never have completed my M.Sc course of the university.

I am highly thankful to all my colleagues: Fayaz Ahmad, Bilal Malik, Khalid Sultan, Sheikh Ansar, Waseem Raja, Firdous Ahmad, Naveel, Zahoor Ahmad and Asloob Rather with whom I shared my joyful memories. My special thanks go to my seniors, Raja Nisar, Shabir Ahmad, Asif Iqbal, Waheed and Gowher Hussain for their constant help and encouragement.

In addition, I would also like to thank my childhood friends Reyaz Ahmad, Hilal and Mohd. Sayeed who made my life interesting and colourful.

Lastly, I alone assume full responsibility for any errors or inadequacies, if present.

.

Sajad Hussain Bhat

Post Graduate Department of Physics, University of Kashmir, Srinagar.

Certificate

This is to certify that the dissertation entitled "***Studies on the Composition, Distribution and Detection of Dark matter in the universe***" submitted by ***Sajad Hussain Bhat***, in partial fulfillment for the award of the degree of ***Master of Philosophy*** in ***Physics***, is the original research work carried out by him under my supervision and guidance. It is further certified that the dissertation has not been submitted for the award of M. Phil. or any other degree to this University or any other University. The scholar has attended the department for statutory period as required under rules.

Dr. Manzoor A. Malik
(*Supervisor*)

Dr. Manzoor A. Malik
(*Head of the department*)

Contents

List of Figures

List of Tables

Chapter 1

General Introduction

Dark matter is the unseen matter that, unlike the visible matter, does not emit any electromagnetic radiation. The discovery of dark matter is of fundamental importance for both particle physics and cosmology. Astrophysical observations such as the rotational curves in galaxies, the gravitational lensing of galactic clusters, the WMAP Cosmic Microwave Background anisotropy measurements and the simulations for large scale structures of the universe have indicated that nearly 23 % of the energy density of our universe is made of non-baryonic cold dark matter, while only 4 % is made of ordinary baryonic matter. The origin and the nature of dark matter, however, remains largely unknown, which is a great challenge of our time. From particle physics point of view, the existence of dark matter definitely requires new physics beyond the current standard model of particle physics. General relativity, astrophysics, and cosmology dictate how dark matter acts on large-scales and how the Universe may be viewed as a laboratory to study dark matter. Many other areas of physics come into play as well, making the study of dark matter a diverse and interdisciplinary field.

Some excellent recent reviews [1, 2, 3] describe the current status of dark matter research in detail. The first sign of the existence of dark matter was an inference of the work of Oort [4], who found that the motion of stars in the Milky Way is suggestive of the presence of far more galactic mass than anyone had previously predicted. By studying the Doppler shifts of stars moving near the galactic plane, Oort was able to calculate their velocities, and thus made the startling discovery that the stars should be moving quickly enough to escape the gravitational pull of the luminous mass in the galaxy. Oort postulated that there must be more mass present within the Milky Way to hold these stars

in their observed orbits. However, Oort noted that another possible explanation was that 85% of the light from the galactic center was obscured by dust and intervening matter or that the velocity measurements for the stars in question were simply in error [4].

Coinciding with the Oort's discovery, Swiss astronomer Zwicky found similar indications of missing mass, but on a much larger scale [5]. While measuring radial velocities of member galaxies in the Coma cluster (that contains some 1000 galaxies), and the cluster radius from the volume they occupy, Zwicky used the virial theorem to infer the existence of unseen matter. His calculations yielded a value about 160 times greater than expected from their luminosity. Zwicky concluded that, the cluster will be bound only if it contains dark matter in large quantities [5]. His suggestion was not taken seriously at first by the astronomical community until about forty years later when studies of motions of stars within galaxies also implied the presence of a large halo of unseen matter extending beyond the visible stars.

Following the discoveries of Oort, Zwicky, and others, Vera Rubin and collaborators conducted a detailed study of the rotation curves of 60 isolated galaxies [6]. Since the stars in distant galaxies are simply too faint, so Rubin used clouds of gas rich in hydrogen and helium that surround hot stars as tracers of the rotational profile. With the help of new sensitive detectors, Rubin et al. measured the velocity of hydrogen gas clouds in and near the andromа galaxy. These hydrogen clouds orbit the galaxy much as stars orbit with in the galaxy. They expected that the hydrogen gas outside the visible edge of the galaxy would move slower than the gas at the edge of the galaxy but they found that the orbital velocities of hydrogen clouds remain constant outside the visible edge of the galaxy. To explain this they argued that, if the stars inside the andromа galaxy obey newtons laws then their orbital speeds can be expressed as:

$$V(r) = \sqrt{\frac{Gm(r)}{r}} \tag{1.1}$$

where $v(r)$ is the orbital speed of the object at a radius r, G is the gravitational constant, and $m(r)$ is the total mass contained within r, which is derived from simply setting the gravitational force equal to the centripetal force. Therefore, $v(r) \propto \frac{1}{\sqrt{r}}$ meaning that the velocity of a rotating body should decrease as its distance from the center increases, which is generally referred to as the Keplerian behavior. Rubin's results showed an extreme deviation from predictions due to Newtonian gravity and the luminous matter distribution, i.e the rotation curves of stars are flat. (A typical rotation curve of dwarf spiral galaxy M33

is shown in figure 1.1). They concluded that there exists non-luminous mass inside the galaxy which is responsible for the flatness of the rotation curves.

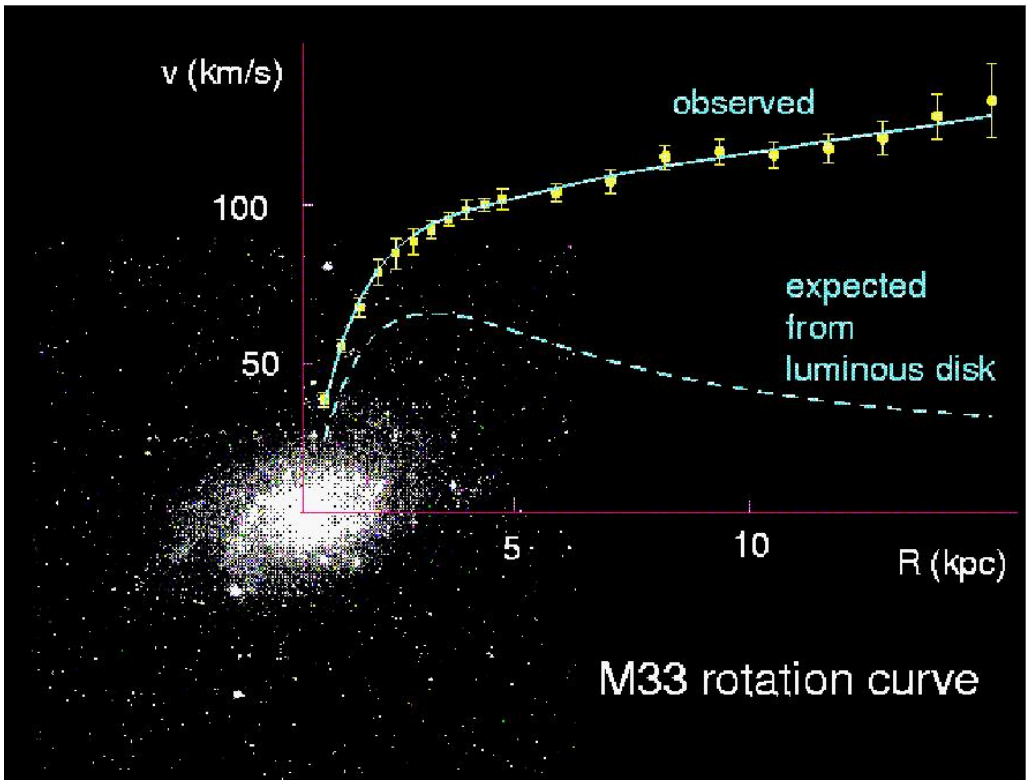

Figure 1.1: The observed rotation curve of dwarf spiral galaxy M33 compared to an idealized Keplerian behavior [7].

Gravitational lensing as a tool to probe the amount and distribution of dark matter was discovered in the 1970's. Gravitational lensing is a result of Einstein's Theory of Relativity which postulates that the Universe exists within a flexible fabric of space time. Objects with mass bend this fabric, affecting the motions of bodies around them. In a gravitational lensing system light from a distant object (the source) is deflected by the gravitational potential of an intervening object (the lens) on its way to the observer. If the distant galaxy were to be located directly behind the cluster, a complete Einstein ring would appear; this looks much like a bulls eye, where the center is the closer object and the ring is the lensed image of the more distant object. However, the likelihood of two

appropriately bright and distant objects lining up perfectly with the Earth is low; thus, distorted galaxies generally appear as arclets, or partial Einstein rings.

The first gravitational lensing event was discovered by Walsh et al. in 1979. While working at the Kitt Peak National Observatory, they found two distant objects separated by only 5.6 arc seconds with very similar red shifts, magnitudes, and spectra [8]. They concluded that perhaps they were seeing the same object twice, due to the lensing of a closer massive object. Similar observations were made by Lynds and V. Petrosian in 1988, in which they saw multiple arclets within clusters [9].We can study a distant galaxy's distorted image and make conclusions about the amount of mass within a lensing cluster using this expression for θ_E, the Einstein radius (the radius of an arclet in radians)

$$\theta_E = \sqrt{\frac{4GMd_{LS}}{c^2 d_L d_s}} \tag{1.2}$$

where G is the gravitational constant, M is the mass of the lens, c is the speed of light, and d_{LS}, d_L, and d_S are the distance between the lens and source, the distance to the lens, and the distance to the source, respectively (these distances are angular-diameter distances). Physicists have found that this calculated mass is much larger than the mass that can be inferred from a cluster's luminosity. For example, for the lensing cluster Abell 370, Bergmann, Petrosian, and Lynds [10] determined that the M/L ratio of the cluster must be about $10^2 - 10^3$ solar units, necessitating the existence of large amounts of dark matter in the cluster as well as placing constraints on its distribution within the cluster [1, 10].

1.1 Evidences for the Existence of Dark Matter

After giving a brief description of the historical developments towards the understanding of dark matter problem in physics, we will now move towards some more exciting evidences which will substantiate our claim that Dark matter exists in our universe.

1.1.1 Cosmological Evidence

According to the Big bang model, the universe began in an extremely hot and dense state. It is that epoch when the neutrons and protons fused together to form deuterium, helium, and trace amounts of lithium and other light elements. This process of element

formation is known as nucleosynthesis. In fact, BBN (Big Bang Nucleosynthesis) is the largest source of deuterium in the Universe as any deuterium found or produced in stars is almost immediately destroyed (by fusing it into ^4He); thus the present abundance of deuterium in the Universe can be considered a lower limit on the amount of deuterium created by the Big Bang. Therefore, by considering the deuterium to hydrogen ratio of distant, primordial-like areas with low levels of elements heavier than lithium (an indication that these areas have not changed significantly since the Big Bang), physicists are able to estimate the D/H abundance directly after BBN. Using nuclear physics and known reaction rates, BBN elemental abundances can be theoretically calculated. The precise agreement between theory and observational determinations of these light elemental abundances is considered as a success of the Big Bang theory. Figure 1.2 shows theoretical elemental abundances as calculated with the BBN code $nuc123$ compared with experimental ranges[11]. It turns out that the D/H ratio is heavily dependent on the overall density

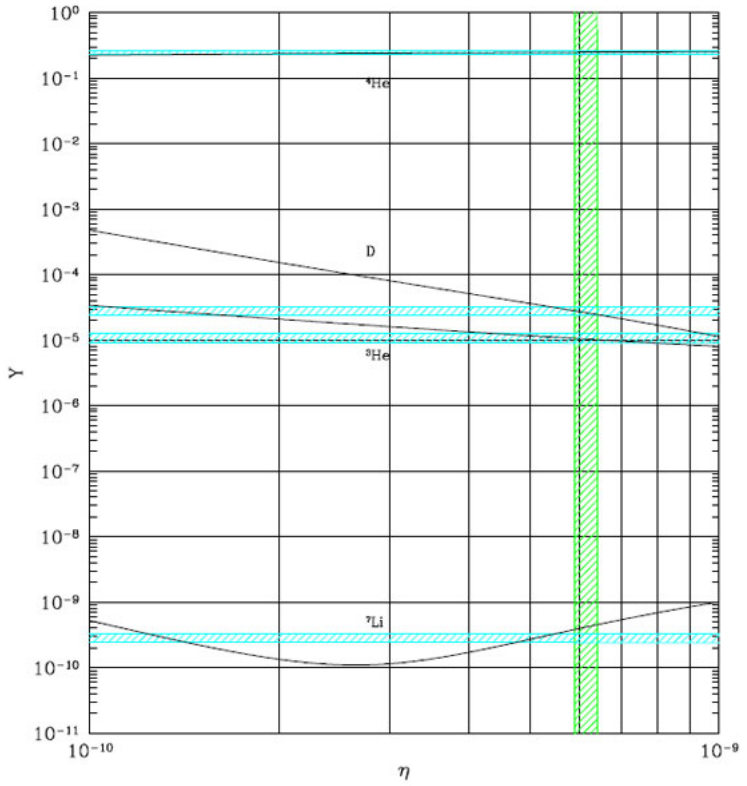

Figure 1.2: Light elemental abundances versus the photon to baryon ratio, η. The horizontal lines show measured abundances of the respective elements and the vertical lines show the photon to baryon ratio as measured by WMAP [11].

of baryons in the Universe, so measuring the D/H abundance gives the overall baryon

abundance. This is usually represented by $\Omega_b h^2$, where Ω_b is the baryon density relative to a reference critical density (ρ_c) and $h = H/100\ kmsec^{-1}Mpc^{-1}$ (the reduced Hubble constant, which is used because of the large historical uncertainty in the expansion rate of the Universe). Cyburt [12] calculated two possible values for $\Omega_b h^2$ depending on what deuterium observation is taken: $\Omega_b h^2 = 0.0229 \pm 0.0013$ and $\Omega_b h^2 = 0.0216^{+0.0020}_{-0.0021}$, both which we will see accounts for only about 20% of the total matter density [1, 12].

The cosmic microwave background radiation (CMB), discovered in 1965 by Penzias and Wilson as an excess background temperature of about 2.73 K, is another way through which we can describe the composition of the Universe [13]. Most of the cosmological information we get from the CMB is found by studying its power spectrum, a plot of the amount of fluctuation in the CMB temperature spectrum at different angular scales on the sky. One of the cornerstones of Big Bang Cosmology was the prediction of anisotropies (variation in temperature from one part of the microwave sky to another) in the cosmic microwave background. The COBE (COsmic Background Explorer) satellite's DMR instrument first detected these anisotropies at the level of 1 part in 10^5 [14]. Since these temperature anisotropies are related to the density fluctuations, CMB anisotropy reveals a wealth of information about the origin and evolution of the structures (Galaxies, Clusters etc) that we see in the Universe today. The origin of structures that we see today is still being debated. However, a very simple and plausible explanation is as follows: Structures formed because gravity pulled together matter that existed originally in slightly denser regions. Given the attractive nature of gravitational force, more and more matter was pulled in with the passage of time making compressed and denser structures until galaxies and other objects resulted. These objects resist further collapse because of their rotation and/or internal motions. While as it is widely believed that this gravitational instability is responsible for the formation of structures that we see today, it requires small initial density fluctuations to start the process of collapse. These density fluctuations are imprinted on the CMB temperature anisotropies. Owing to the significance of an accurate measurement of these anisotropies, a number of ground based, balloon borne and satellite experiments were performed (some in progress) so as to measure these anisotropies with improved angular resolution and sensitivity. These anisotropies can be expressed by using a spherical harmonic expansion of the CMB sky. The improved resolution anisotropy map of the sky as observed by WMAP (7 year) is shown in figure (1.3).

As shown in the figure, the fluctuation spectrum is flat upto $l \approx 30$ rises to a clear peak at $l \approx 200$, followed by a lower amplitude second peak, third peak, higher or-

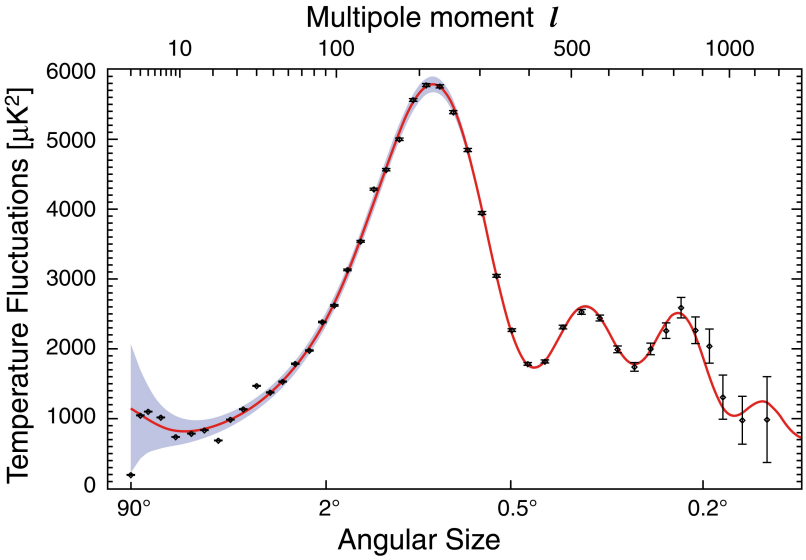

Figure 1.3: The 7-year temperature (TT) power spectrum from WMAP. The gray band represents cosmic variance. (Figure credit: WMAP science team)

der peaks and a damping tail. These peaks in the power spectrum are called 'Acoustic Peaks'. The positions and magnitudes of the peaks contain fundamental properties about the geometry and structure of the Universe. For example, the first peak tells us that the curvature of the Universe is close to 'flat'. The reason for this peak is that sound waves of the right frequency would have had just enough time to reach maximum compression when the Universe became transparent. The ratio of second to first peak amplitude gives the ratio of the baryon density to the critical closure density. The result from the WMAP 7 year data [15] is $\Omega_b = 0.0449 \pm 0.0028$. The third acoustic peak and the onset of the Silk damping tail are now well measured by WMAP. The third peak helps us to estimate the total matter density relative to critical density from which it follows that the Dark Matter density is 0.222 ± 0.026 [15].

The first essential observation is that these two numbers are different; baryonic matter is not the only form of matter in the Universe. In fact, the dark matter density is around 83% of the total mass density. Locally, this corresponds to an average density of dark matter $\rho_{dm} \approx 0.3 GeV/cm^3 \approx 5 \times 10^{-28} kg/m^3$ at the Sun's location. An analysis of the CMB allows for a discrimination between dark matter and ordinary matter precisely because the two components act differently; the dark matter accounts for roughly 85% of the mass, but unlike the baryons, it is not linked to the photons as part of the photon-baryon fluid. Figure 1.4 demonstrates this point extremely well; small shifts in the baryon

density result in a CMB anisotropy power spectrum which are wholly inconsistent with WMAP and other CMB experiment data.

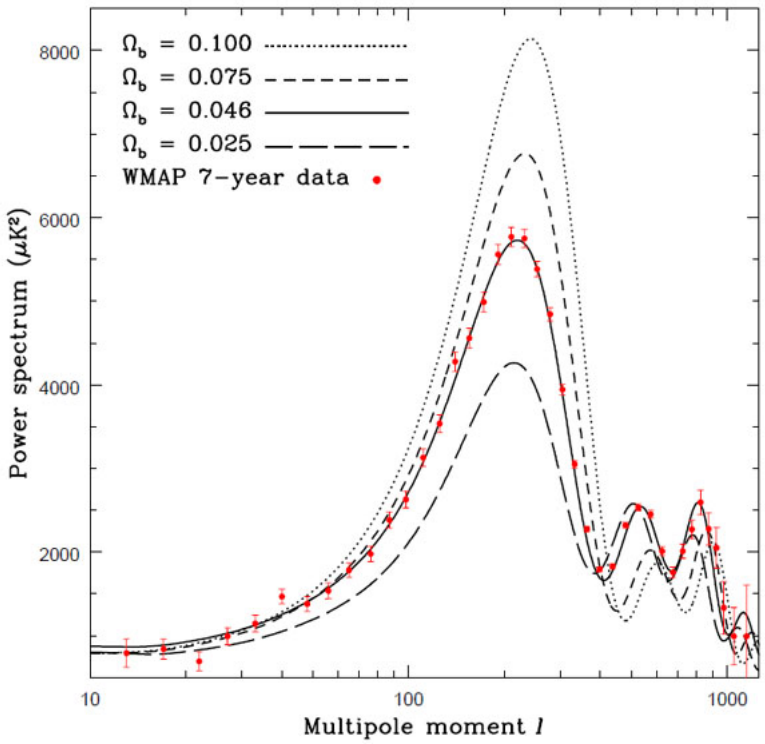

Figure 1.4: The CMB Anisotropy Power Spectrum for various values of Ω_b (holding $\Omega_{tot} = 1$) with WMAP year 7 data. The anisotropy power spectrum gives the level of temperature fluctuations on patches of various angular scales, where a spherical version of a Fourier transform gives multipoles l, where roughly $l = 180^0/\theta$, with θ the angular scale in degrees [15].

Analysis of the large-scale structure of the Universe also yield evidence for dark matter and helps to break degeneracies present in the CMB data analysis. By calculating the distance to galaxies using their redshifts, cosmologists have been able to map out the approximate locations of more than 1.5 million galaxies. For example, the Sloan Digital Sky Survey (SDSS) has created 3D maps of more than $900,000$ galaxies,$120,000$ quasars, and $400,000$ stars during its eight years of operation [16]. In fact, galaxy counts have had a long and important history in cosmology; in the 1950s and 60s radio galaxy counts provided the earliest, hard evidence against the Steady State model. But how can galaxy counts give evidence for dark matter? As discussed earlier, the current structure in the Universe is due to initial density fluctuations which served as seeds for structure

formation magnified by the presence of dark matter. The most likely source of these initial density perturbations are quantum fluctuations magnified by inflation, a period of early rapid exponential growth approximately 10^{-35} seconds after the Big Bang. Under the assumption that these random fluctuations are Gaussian, a single function, the power spectrum $P(k)$, is sufficient to describe the density perturbations. From here a given $P(k)$ can be used to theoretically calculate large scale structure. Furthermore, the converse is also true: by measuring large-scale structure (galaxy counts and surveys) one can experimentally determine the power spectrum $P(k)$. The peak of $P(k)$ is sensitive to the value of Ω_m, and the amount of baryons has effects on the shape of $P(k)$ (through baryonic acoustic oscillations, that is, excesses in galaxies separated at certain distances due to sound waves in the pre-recombination plasma)[17]. Using these techniques, a final study of the 2dF Galaxy Redshift Survey power spectrum found $\Omega_m = 0.231 \pm 0.021$ and $\Omega_b/\Omega_m = 0.185 \pm 0.046$; a study based on data from SDSS yielded $\Omega_m = 0.286 \pm 0.018$ and $\Omega_{dm}h^2 = 0.02267 \pm 0.00058$ [18, 19]. Note that these results agree with both CMB and BBN predictions.

Recently, Evoli et al [20] used strategy based on the search for the imprints left on the CMB temperature and polarization spectra by the energy deposition due to annihilations of the most promising dark matter candidate, a stable WIMP of mass 1-20 GeV. They found that the strongest constraints are obtained from Monte Carlo Markov Chains analysis of the combined WMAP7 and SPT datasets up to $l_{max} = 3100$. If annihilation occurs via the $e^+ - e^-$ channel, a light WIMP can be excluded at $2 - \sigma$ c.l. as a viable DM candidate in the above mass range. However, if annihilation occurs via $\mu^+ - \mu^-$ or $\tau^+ - \tau^-$ channels then WIMPs with mass $> 5GeV$ might represent a viable cosmological DM candidate.

N-body simulations of large-scale structure are another tool which have been used to demonstrate the need for dark matter. These simulations often take weeks to complete on super clusters; for example, MS-II tracked over 10 billion particles which each represent $6.89 \times 10^6 h^{-1} M\odot$ in a volume of $(100h^{-1}Mpc)^3$ to study dark matter halo structure and formation [21]. Similarly, Di Matteo et al. ran simulations to study the role of black holes in structure formation using $20 - 200$ million particles in a volume of $(33.75h^{-1}Mpc)^3$ to $(50h^{-1}Mpc)^3$[22]. N-body simulations confirm the need for dark matter. Simulations without dark matter do not form the familiar filament and void-type structures seen in the observable universe by SDSS and other surveys on the proper timescales. Other studies [23, 24] reveal that not only is dark matter needed, but dark matter must be cold or non

relativistic during the period of structure formation.

1.1.2 Microlensing

Microlensing refers to the special case of gravitational lensing where the multiple images produced are too close together on the sky to be observed as separate images. However, the lensing can still be detected because these multiple objects appear as a single object of increased apparent brightness. The major application of microlensing suggested by Paczynski in 1986 [25], is the search for baryonic dark matter candidates known as MACHOs (Massive Astrophysical Compact Halo Objects). Many experiments, in particular, the MACHO Collaboration [28] and the EROS-2 Survey [29], have investigated for gravitational microlensing caused by possible MACHOs in the Milky Way halo. Search for MACHOs has also been carried out by other groups such as MOA, OGLE, and Super MACHO [26, 27]. The MACHO Collaboration studied 11.9 million stars with only 13-17 possible lensing events detected [28]. The EROS-2 Survey reported even fewer events, observing a sample of 7 million bright stars with only one lensing candidate found [29]. This low number of possible MACHOs can only account for a very small percentage of the nonluminous mass in our galaxy, revealing that most of dark matter can not be baryonic in nature.

1.1.3 Miscellenous Evidences

One way to study the overall properties of dark matter is by analyzing collisions between galaxy clusters, the largest structures in the universe. One such collision event called the “Bullet Cluster” resulting from the collision of two enormous clusters of galaxies had created a lot of excitement in the Dark Matter community. The speed and shape of the bullet, and other information from various telescopes suggest that the smaller cluster passed through the core of the larger one about 150 million years earlier. The force of this collision event between two massive clusters (Figure 1.5) was so great that it wrenched the ’normal’ matter in the form of hot gas (seen in pink) away from the dark matter (blue). However, the majority of a clusters baryonic mass exists in the extremely hot gas between galaxies, and the cluster collision compressed and shock heated this gas; as a result, a huge amount of X-ray radiation was emitted. Comparing the location of this radiation (an indication of the location of the majority of the baryonic mass in the clusters) to a

mapping of weak gravitational lensing (an indication of the location of the majority of the total mass of the clusters) shows an interesting discrepancy; the areas of strong X-ray emission and the largest concentrations of mass seen through gravitational lensing are not the same. The majority of the mass in the clusters is non baryonic and gravity points back to this missing mass [30].

Figure 1.5: This image of the Bullet cluster shows a separation of dark matter from the luminous matter, with the dark matter shown in blue and the luminous matter shown in red. (Image credit: X-ray: NASA/CXC/CfA/M.Markevitch et al.)

Bradac et al. [31] studied another powerful galaxy cluster collision (MACS J0025.4-1222) and found that the behavior of the matter within this cluster is strikingly similar to the Bullet Cluster; the dark matter passed through the collision while the intergalactic gas interacted and emitted X-rays. These results reaffirmed those of the Bullet Cluster and the need for collision less dark matter.

A ring-like structure of dark matter, caused by cluster collision was reported by NASA's Hubble Space Telescope in 2007. Initial detections of dark matter in the cluster, made in 2007, were so unusual that astronomers shrugged them off as unreal, because of poor data. New results from NASA's Hubble Space Telescope [32] confirm that dark matter and galaxies separated in Abell 520.

Penny et al. [33] studied the structure and dark matter content of cluster dwarf spheroidals using Hubble space telescope data involving 29 dwarfs as cluster members,

17 of which were previously unstudied. The dwarfs in their study were found to be very smooth with very low asymmetry and clumpiness, throughout their entire structure, showing no evidence for internal features or star formation that could be the result of tidal processes or star formation induced by the cluster environment. Based on these observations, and the sizes of these dwarfs, they argued that some of the dwarfs in their sample must have a large dark matter content to prevent disruption by the cluster potential.

A new approach to the indirect detection of dark matter called the 'General Antiparticle Spectrometer' (GAPS) has recently been proposed [35] . It relies on searching for primary antideuterons produced in the annihilation of dark matter in the galactic halo. Low energy antideuterons produced through Standard Model processes, such as collisions of cosmic-rays with interstellar baryons, are greatly suppressed compared to primary antideuterons. Thus a low energy antideuteron search provides a clean signature of dark matter. In GAPS antiparticles are slowed down and captured in target atoms. The resultant exotic atom deexcites with the emission of X-rays and annihilation pions, protons and other particles. A tracking geometry allows for the detection of the X-rays and particles, providing a unique signature to identify the mass of the antiparticle. There are also indications that dark matter candidates with electromagnetic dipole moments can arise as dark baryons in guage-mediated models. Banks et al [36] claim that significant direct detection signals can arise from dipolar dark matter with mass on the order of tens of TeV.

The point we are trying to make is that there are ample evidences which support the existence of Dark matter and a lot of progress has been made on indirect as well as direct detection of Dark Matter. However, the nature and amount of Dark matter that is present in our universe remains an open question. Knowing the right amount of Dark matter will decide the fate of our universe i,e whether our universe is flat, open or closed. For this purpose we will first discuss the energy density of our universe.

1.2 Energy density of our universe

The overall composition of our universe can be described by the density parameter Ω, defined as the average energy density of the universe ρ relative to the critical density

needed for a spatially flat universe. From the Einstein's field equations:

$$\left(\frac{\dot{R}}{R}\right)^2 = \frac{8\pi G\rho}{3} - \frac{k}{R^2} + \frac{\lambda}{3} \tag{1.3}$$

The Hubble constant can be written as

$$H = \frac{\dot{R}}{R}, \tag{1.4}$$

such that from equation (1.3) we get

$$H^2 = \frac{8\pi G\rho}{3} - \frac{k}{R^2} + \frac{\lambda}{3} \tag{1.5}$$

where $R(t)$ is the cosmological scale factor, k is the constant which determines the geometry of the universe ($k = 0,\ +1,\ -1$ gives flat, closed and open universe respectively) and λ is the cosmological constant which contains contribution from the vacuum energy density. The critical density is defined as

$$\rho_c = \frac{3H_0^2}{8\pi G} \tag{1.6}$$

(H_0 is present value of Hubble constant) Where $H_0 = 100h_o kms^{-1}/Mpc$. The present estimate of h_o lies in the range $0.5 \leq h_o \leq 1$ therefore $\rho_c = 1.88 \times 10^{-29} h_o^2 gcm^{-3}$ (where $h_o = 0.71 \pm 0.01$).

The cosmological density parameter is then defined to be:

$$\Omega = \frac{\rho}{\rho_c} \tag{1.7}$$

we can express the density parameter of universe as:

$$\Omega_T = \Omega_B + \Omega_{DM} + \Omega_\lambda \tag{1.8}$$

The observations of the WMAP Data[37], High red shift supernova type I_a Data[38] and Baryon Acoustic oscillations[39] suggest that

$$\Omega_T = 1.006 \pm 0.006 \tag{1.9}$$

with $h_0 = 0.71 \pm 0.01$, $\Omega_m h_0^2 = 0.133 \pm 0.006$, $\Omega_\lambda = 0.71 \pm 0.03$ and $\Omega_B h_o^2 = 0.0227 \pm 0.0006$. In equation (1.8), Ω_B is the contribution to Ω_T from the baryonic matter, Ω_{DM} is contribution to Ω_T from the Dark matter and Ω_λ is the contribution to Ω_T from the Dark energy.

Based on the above data we can write: $\Omega_m \approx \frac{1}{3}$ and $\Omega_{DE} \approx \frac{2}{3}$. It is to be noted that the nature of neither Dark Matter nor Dark Energy is currently known precisely. It is felt that both Dark matter and Dark Energy are non-baryonic in origin while Dark matter clusters on sub-Megaparsec scales (to explain the rotation curves of galaxies), dark energy has a large negative pressure (leading to an accelerated universe).

It is now clear that the understanding of our universe is far from complete with out the understanding of Dark matter and Dark energy,because Dark matter accounts for 23% of the mass-energy density of the observable universe, while Dark energy accounts for 73% and the ordinary matter accounts for merely 4% of the mass-energy density of observable universe. Understanding dark energy is important in its own right but is not the subject of our present study.

1.3 Particle Physics and Cosmology

While, at the face of it, cosmology and particle physics appear to be incompatible, as cosmology is the study of the universe, where the distance scale involved is many Giga-parsecs and particle physics studies the fundamental constituent of matter, now reaching the distance scale of $\approx 10^{-17} cm$, there is a common meeting ground. Current studies of cosmic microwave background showing that the universe was filled with a hot plasma made of photons, electrons, and nuclei in thermal equilibrium complemented by the Hubble expansion imply that the early universe was hot and compact, in confirmity with the Big Bang theory. Understanding of early stages of the universe requires the development in particle physics, while the universe as a whole may be regarded as a testing ground of hypothesized particle physics at high energies beyond the reach of accelerators. As far as Dark matter is concerned, cosmologists are heavily dependent on particle physicists and therefore the particle physics models that throw light on the Dark matter deserve a mention. In the following subsections, we shall briefly touch the standard model and the SUSY model:

1.3.1 The Standard Model

The standard model (SM) of particle physics is a remarkably successful theory of elementary particles and their interactions. There are sixteen confirmed particles in the SM, seven of which were predicted by the model before they were found experimentally. The discovery of a new subatomic particle that is likely the elusive Higgs boson adds value to the standard model. In a much-hyped announcement, made in July 2012, the LHC scientists reported evidence of a new 'Higgs-like' particle with roughly 125 times the mass of the proton. Higgs is the missing link in the Standard Model of particle physics with even wider implications: It opens the door beyond the Standard Model for explaining the existence of dark matter. Table 1.1 enlists the SM fundamental particles and some of their basic qualities. An excellent introduction to the Standard Model can be found in reference [40].

(a) Fermions

Quarks	Mass (MeV)	Charge	Leptons	Mass (MeV)	Charge
u	2.55	$+2/3$	(e^-)	0.511	-1
d	5.04	$-1/34$	(ν_e)	2.0×10^{-6}	0
c	1270	$+2/3$	(μ)	105.7	-1
s	104	$-1/3$	(ν_μ)	0.19	0
t	171200	$+2/3$	(τ^-)	1776.8	-1
b	4200	$-1/3$	(ν_τ)	18.2	0

(b)Gauge Bosons

Particle	Force	Mass (MeV)	Charge
Photon(γ)	Electromagnetic	0	0
Z boson	Weak interaction	91188	0
boson ($W^\pm$)	Weak interaction	80398	$+1, -1$
Gluon (g)	Strong interaction	0	0
Higgs boson	Higgs field	114400	0

Table 1.1: The particles predicted by the Standard Model[47].

Unfortunately, the SM does not contain any particle that could act as the dark matter. Neutrinos seem to the only possible candidate of dark matter in SM. But there are many issues that dismiss neutrinos as dark matter candidates. Chief reasons against neutrinos are: (a) A neutrino-dominated universe would have inhibited structure formation and caused a top-down formation (larger structures forming first)[43] which is against the

most likely bottom-up formation (stars, galaxies then large galaxies then clusters, etc.) [44]. (b) Spergel et al. have shown that the WMAP data combined with large-scale structure data constrains the neutrino mass to $m_\nu < 0.23eV$, which in turn makes the cosmological density $\Omega_\nu h^2 < 0.0072$ [45]. This implies that while neutrinos can account for a small fraction of dark matter, they cannot be the only source.

Based on very strong theoritical arguments, the standard model of particle physics is now viewed by many as an effective field theory valid for energies up to the TeV scale, rather than a truly fundamental theory. Further, empirical evidences like existance of non-baryonic dark matter, dark energy, neutrino mass etc demonstrate that the standard model is incomplete. Among the proposed extensions of the standard model, supersymmetry (briefly described in the next section) is undoubtedly the most studied, and probably one of the best motivated.

1.3.2 Supersymmetry (SUSY)

The supersymmetric model is a phenomenological model that is specifically tailored to the study of dark matter. There are different versions of the model, one of the most popular being a seven free parameters theory, where all parameters are specified at low energy. A less constrained version of this model has 24 free parameters, which has been used by Bertone [46] to study the complementarity of direct and accelerator searches.

An exhaustive discussion of the SUSY model is beyond the scope of this dissertation. Amsler et al [47] gives an excellent review. Here, we only mention the possible particles which could act as dark matter. These are the neutralino (a particle state which is a superposition of the neutral superpartners of the Higgs and gauge bosons), the sneutrino (the superpartner of the neutrino), and the gravitino (the superpartner of the graviton which would come from a quantum theory of gravity). All of these particles are electrically neutral and weakly interacting, and thus are ideal WIMP-like candidates for dark matter. However, sneutrinos annihilate very rapidly in the early universe, and sneutrino relic densities are too low to be cosmologically significant [51, 52]. And gravitinos act as hot dark matter rather than cold dark matter, and large scale structure observations are inconsistent with a universe dominated by hot dark matter [53, 54]. This leaves the neutralino as a viable candidate.The new particles generated by adding SUSY to the SM are shown in Table 1.2.

(a) Sfermions

Particle	Mass (MeV)	Charge	Particle	Mass (MeV)	Charge
up squark($\tilde{u}$)	> 379	+2/3	selectron($\tilde{e}$)	> 73	-1
down squark($\tilde{d}$)	> 379	$-1/3$	$\tilde{e}$ sneutrino	> 95	0
charm squark($\tilde{c}$)	> 379	$+2/3$	smuon($\tilde{\mu}$)	> 94	-1
strange squark($\tilde{s}$)	> 379	$-1/3$	μ sneutrinos($\tilde{\nu_\mu}$)	> 94	0
top squark($\tilde{t}t$)	> 92.6	$+2/3$	stau($\tilde{\tau}$)	> 81.9	-1
bottom squark($\tilde{b}$)	> 89	$-1/3$	τ sneutrinos($\tilde{\nu_\tau}$)	> 94	0

(b) Gauginos

Particle	Mass (GeV)	Description
Neutralinos ($\tilde{\chi}^0_{1-4}$)	> 46	Mixture of photino($\tilde{\gamma}$),zino($\tilde{Z}$)and neutral Higgsino($\tilde{H}^0$).
Charginos ($\tilde{\chi}^\pm_{1,2}$)	> 94	Mixture of Winos ($\tilde{W}^\pm$) and charged higgsino($\tilde{H}^\pm$).
Gluinos ($\tilde{g}$)	> 308	Superpartner of gluon.

Table 1.2: The particles predicted by a supersymmetric extension of the Standard Model[47].

1.4 Structure of the Dissertation

During the last few decades, it has been discovered that most of the material in the Universe is invisible and it interacts only gravitationally with the rest of the Universe components. From the latest measurements of WMAP satellite we know that the Universe consists of 4% Baryons, 23% Dark Matter, 73% Dark Energy [15].

Now it is a wonderful time to study cosmology. Using the latest technological advances we have obtained detailed picture of the early universe and maps of the distribution of matter on the largest scales in the universe today. We have a physical model for the origin and evolution of the Universe.The indication of the existence of a Higgs like boson from CERN headquarters helps us to understand the process though which particles get mass in a much better way. However there are still lot of problems in physics which are either unexplored or are being presently investigated .The problem of distribution of Dark matter in universe and the prospects of its detection has attracted the attention of Astrophysists and the experts of particle physics from across the globe.The main aim of my M. Phil. dissertation is to present a precise review of the present status of Dark matter problem. The dissertation is organized as under:

- In chapter2, we will explore the Candidates of Dark matter both from the particle

physics and Astrophysics. We will also present the detailed description of Dark matter candidates from supersymmetry(SUSY).

- In chapter3, we will see how dark matter in distributed in our universe. We will discuss the evidences which support the presence of Dark matter in galaxies, Clusters of galaxies and in the super clusters. We will also use some theoretical models to present a thorough study of Dark matter distribution.

- In chapter4, we will discuss the prospects of Dark matter detection. We will also go through the Direct and Indirect methods which are being employed for the detection of Dark matter.

- In chapter5, we will give a summary of the work presented in this dissertation and point out some main conclusions. Future outlook is also given.

Chapter 2

Candidates for Dark Matter

2.1 Introduction

The existence of Dark Matter is now fairly established even though we have only indirect evidences. However, there is no consensus on the composition of dark matter. The potential candidates for Dark Matter must satisfy the condition that they must be stable on cosmological time scales and must have the right relic cosmological density [55]. An enormous number of candidates have been proposed with masses ranging from $10^{-4}eV$ (axions) up to 10^4 Solar Mass (black holes). Even there is no general consesus on the categorization scheme. The one commonly followed makes a distinction between the baryonic and non-baryonic dark matter. The main baryonic candidates are Massive Astrophysical Compact Halo Objects (MACHOs), which include Brown Dwarfs, White Dwarfs, Neutron stars and Black Holes. The non-baryonic candidates are furthur classified into Hot Dark matter and Cold Dark matter. The neutrino is the most discussed candidate in the Hot Dark matter catagory, while the Cold Dark matter includes the supersymmetric partners of the Standard Model particles usually called as WIMPs (Weakly Interacting Masssive Particles). The WIMPs are comprised of, Neutalinos, sneutrinos, heavy fourth-generation Dirac and Majorana neutrinos, and Axions. Current understanding (though poor) indicates that Dark matter should be in the form of some non-luminous, non-baryonic, non-relativistic, and collisionless elementary particles that have not yet been discovered. However, for the sake of completeness we have also briefly described the baryonic candidates.

In this chapter we will present some most motivated and studied candidates for Dark

matter. Most of them are non-baryonic and non-relativistic particles. However, some relativistic particles and baryonic objects could also be (part of) Dark Matter.

2.2 Cold Dark Matter (CDM)

Cold has been used here to indicate that such Dark Matter particles moved non relativistically at the matter-radiation decoupling time in the early Universe [56], i.e., at the time in which galaxies could just start to form. Due to their relatively slower velocities Cold Dark Matter would first form some relatively small galactic scale structures; large galaxies and clusters of galaxies are formed through hierarchical merging of these smaller structures.

2.2.1 Weakly Interacting Massive Particles (WIMPs)

Weakly Interacting Massive Particles (WIMPs) χ arise e.g. in supersymmetric extensions of the Standard Model of electroweak interactions and are the leading non-baryonic candidates for Cold Dark Matter [57]. They are stable particles and interact with ordinary matter only via weak interactions. Typically their masses have been presumed to be between 10 GeV and a few TeV [57]. They could include Neutralinos, sneutrinos, heavy fourth-generation Dirac and Majorana neutrinos, and Axions [57].

Relic elementary particles are left over from the Big Bang. Stable or long-lived particles with very weak interactions can remain in sufficient numbers to account for a significant fraction of critical density [59]. Very weak interactions are necessary for their annihilations to cease before their numbers are too small [59].

WIMPs exist in thermal equilibrium and in abundance in the early Universe, when the temperature of the Universe T exceeds their masses $m_\chi (T \geq m_\chi)$ [57]. The equilibrium abundance is maintained by pair annihilation of WIMPs with their antiparticles $\bar{\chi}$ into lighter particles l (quarks and leptons, or even gauge and Higgs-bosons if their masses are heavy enough) and vice versa $(\chi\bar{\chi} \leftrightarrow l\bar{l})$ [57]. The rate of this reaction is proportional to the product of the WIMP number density n_χ and the WIMP pair annihilation cross section into SM particles σ_A times the relative velocity between the two WIMPs in their center of mass system v [57].

$$\Gamma_\chi = n_\chi \langle \sigma_A v \rangle \tag{2.1}$$

where $\langle \sigma_A v \rangle$ indicates the thermal averaging.

As the Universe cools to a temperature less than the masses of WIMPs ($T < m_\chi$), the equilibrium abundance (number density) of WIMPs drops exponentially until the rate for the annihilation reaction ($\chi\bar{\chi} \rightarrow l\bar{l}$) becomes smaller than the Hubble expansion rate of the Universe ($\Gamma_\chi \leq H$). At this point the interactions which maintain thermal equilibrium freeze out and the WIMPs cease to annihilate and drop out of thermal equilibrium [55]. Hence, a relic cosmological abundance freezes [57] i.e., the density of the co-moving WIMPs remains essentially constant.

The time evolution of the number density of WIMPs $n_\chi(t)$ can be described by the Boltzmann equation [57]:

$$\frac{dn_\chi}{dt} + 3Hn_\chi = -\langle \sigma_A v \rangle [n_\chi^2 - (n_\chi^{eq})^2] \tag{2.2}$$

Here n_χ^{eq} is the number density of WIMPs in thermal equilibrium. The second term on the left-hand side accounts for the expansion of the Universe, the first term in the brackets on the right-hand side accounts for the depletion of WIMPs due to their pair-annihilation, and the second term arises from creation of WIMPs from the inverse reaction [57].In the absence of number changing interactions, the right-hand side would be zero and we would find

$$n \propto \frac{1}{R(t)^3} \tag{2.3}$$

where $R(t)$ is the scale factor of the Universe.

Note that Eq.(2.2) describes both Dirac particles as well as Majorana particles [57], which are particles that themselves are also their antiparticles, such as Neutralinos ($\chi = \bar{\chi}$) [57]. For the case of Majorana particles (they are so-called self-annihilating), the annihilation rate in Eq.(2.1) should be modified to[57]:

$$\Gamma_\chi = (\frac{n_\chi}{2}) \langle \sigma_A v \rangle \tag{2.4}$$

However, in each annihilation, two particles are removed and the factor of 2 can be canceled. For Dirac particles with no particle-antiparticle asymmetry, i.e.$n_\chi = n_{\bar{\chi}}$.Eq.(1) is true. But the total number of particles plus antiparticles must be $2n_\chi$ [57]. In the case of Dirac particles with a particle-antiparticle asymmetry, the relic abundance is generally that given by the asymmetry [57]. For example, the relic proton density is fixed by the

proton-antiproton asymmetry, i.e., the baryon number of the Universe [57].

The early Universe is radiation dominated and the Hubble expansion rate falls with temperature as [57]:

$$H(T) = 1.66(\frac{g_*^{\frac{1}{2}} T^2}{M_{P_{PI}}}) \tag{2.5}$$

Here M_{PI} is the plank mass.

$$M_{PI} = \sqrt{\frac{\hbar c}{G_N}} = 1.2209 \times 10^{19} GeV/c^2 = 2.1764 \times 10^{-5} g. \tag{2.6}$$

and the quantity $g*$ is the effective number of relativistic degrees of freedom. It is approximately equal to the number of bosonic relativistic degrees of freedom plus $\frac{7}{8}$ times the number of fermionic relativistic degrees of freedom [57]. While, for very high temperature($T \geq m_\chi$) [57],

$$n_\chi^{eq} \propto T^3 \tag{2.7}$$

Hence, the expansion rate H(T) in Eq.(2.5) decreases less rapidly than the number density of WIMPs. This means that, at early times, the expansion term in Eq.(2.2), $3Hn_\chi$, is negligible compared with the right-hand side, and the number density tracks its equilibrium abundance [57].

However, at later times or at low temperatures ($T \leq m_\chi$), the right-hand side in Eq.(2.2) becomes negligible compared with the expansion term, and the co-moving abundance of WIMPs remains unchanged [57]. It can be found that [57]:

$$n_\chi^{eq} = g(\frac{m_\chi T}{2\pi})^{\frac{3}{2}} e^{\frac{-m_\chi}{T}}, \tag{2.8}$$

where g is the number of internal degrees of freedom of the WIMPs and thus their density is Boltzmann suppressed [57]. If the expansion of the Universe were so slow that thermal equilibrium was always maintained, the number of WIMPs today would be exponentially suppressed (essentially, there would be no WIMPs) [57]. The temperature T_F which the WIMPs freeze out is given by $\Gamma_\chi(T_F) = H(T_F)$ [57]. Using typical weak-scale numbers, the freeze-out temperature turns out to be [57]

$$T_F \simeq \frac{m_\chi}{20} \tag{2.9}$$

There is a small logarithmic dependence on the mass and annihilation cross section here [57]. As stated above, after freeze out, the abundance of WIMPs per co-moving volume remains constant.

Finally, the present relic density of WIMPs is then approximately given by (ignoring logarithmic corrections) [57]:

$$\Omega_\chi h^2 \simeq const. \times \frac{T_0^3}{M_{PI}^3 \langle \sigma_A v \rangle} \simeq \frac{0.1 cpb}{\langle \sigma_A v \rangle} = \frac{3 \times 10^{-27} cm^3/s}{\langle \sigma_A v \rangle} \tag{2.10}$$

where $T_0 = (2.725 \pm 0.001)K$ is the current CMB temperature and c is the speed of light. It is inversely proportional to the annihilation cross section of WIMPs. Hence, as the annihilation cross section is increased, the WIMPs stay in equilibrium longer, and we are left with a smaller relic abundance [57]. The annihilation cross section is generally expected to decrease as the WIMP mass is increased, so the relic abundance should be also increased [57]. Therefore, heavier WIMPs should be more likely to contribute too much to the mass of the Universe, and then be cosmologically inconsistent [57].

2.2.2 Neutralinos

The favored supersymmetric dark matter candidate is the lightest neutralino; these are the four spin 1/2 Majorana fermion superpartners of the neutral gauge and Higgs bosons (usually denoted χ^0_{1-4}). Similarly, there are two charged Dirac fermion superpartners of charged gauge and Higgs bosons, the Charginos $\chi^\pm_{1-2}$. The successes of supersymmetric models depend on the fact that the Gauginos have weak-scale masses, thus the proper relic density for any stable states comes essentially for free.

The Neutralinos are linear combinations of photino, Z-ino and neutral higgsinos (the supersymmetric partners of the photon, Z^0 and neutral Higgs bosons:

$$\bar{\chi}^0_i = a_i \bar{\gamma} + b_i \bar{Z} + c_i \bar{h}^0 + d_i \bar{H}^0, i = 1, 2, 3, 4 \tag{2.11}$$

In most SUSY models, the lightest neutralino is the lightest supersymmetric particle [55] and therefore the best motivated and the most widely studied candidate for WIMP Dark Matter, but not the unique candidate for LSP (e.g., sneutrinos)[55].

There are some theoretical reasons to believe that the lightest neutralino should be the LSP. First, suppose a charged uncolored SUSY particle, such as a chargino or a slep-

ton, were the LSP. The relic number density of such particles can be given as roughly $10^{-6} n_b M/GeV$ [57], where n_b is the baryon number density and M is the mass of such particles. Then they would show up in searches for anomalously heavy protons [57]. Null results from such searches rule out such charged particles over a broad mass range [57]. Moreover, grand unified models predict relations between the masses of the SUSY particles . In most models the gluino is more massive than the neutralino, and the squarks are also heavier than the sleptons [57]. In addition, some detailed calculations show that the lightest neutralino has the desired thermal relic density, Ω_{DM} , in at least four distinct regions of parameter space [57].

2.2.3 Sneutrinos

Sneutrinos are the spin-0 supersymmetric partner of the neutrinos. There are some reasons to rule out sneutrinos to be good candidate for Dark Matter. First, in most models, there is an slepton with mass similar to, but slightly smaller than, the sneutrino mass [57]. Meanwhile, their masses would have to exceed several hundred GeV for them to make good Dark Matter candidates. This is uncomfortably heavy for the lightest sparticle [55]. On the other hand, the annihilation cross sections of sneutrinos are expected to be quite large [55]. Hence, the negative outcome of various WIMP searches rules out ordinary sneutrinos as primary component of the Dark Matter halo of our Galaxy [55]. However, in models with gauge-mediated SUSY breaking the lightest messenger sneutrino could be a good candidate [55].

2.2.4 Heavy fourth-generation Dirac and Majorana neutrinos

They are the first proposed WIMP candidates for CDM [57]. They are heavy, but stable particles and assumed to have (weak) interactions with ordinary matter through Standard Model coupling to the Z^0 boson [57]. Such neutrinos could annihilate into light fermions via s-channel exchange of a Z^0 boson. For $m \ll M_Z$ the cross section is proportional to the square of their mass [57]. Because their interactions are fixed by gauge symmetry, the only adjustable scale is then their masses [57]. The cosmological abundances of the heavy Dirac and Majorana neutrinos have been given as [57]:

$$\Omega_{\nu,D} h^2 \simeq (\frac{m_{\nu,D}}{2GeV})^{-2} \tag{2.12}$$

and

$$\Omega_{\nu,M}h^2 \simeq (\frac{m_{\nu,M}}{5GeV})^{-2} \tag{2.13}$$

for neutrino masses in the range of $1GeV \leq m_\nu \ll m_Z = 91.19GeV$.

However, there is no obvious reason why such massive neutrinos should not be allowed to decay [55]. Moreover, an SU(2) doublet neutrino will have a too small relic density if its mass exceeds $M_Z/2$, as required by LEP data [55].

On the other hand, for such neutrinos with masses greater than the electroweak gauge-boson masses, annihilations into gauge- and or Higgs-boson pairs could occur. However, the cross section would not decrease as the neutrino mass increases [57], so the relic abundance of neutrinos with masses of the order of $100GeV$ remains too small to account for the Dark Matter in the Galactic halo [57].

Dirac neutrinos interact with nuclei through a coherent vector interaction [57]. Thus the Dirac-neutrino-nucleus cross section is expected to be quite substantial [57], and this would lead to a significant event rate in a direct detection experiment. The results from such experiments have ruled out Dirac neutrinos with masses in the range $12GeV \leq m_{v,D} \leq 1.4TeV$ as the primary component of the Dark Matter halo [57].

Meanwhile, Majorana neutrinos interact with nuclei only via an axial-vector interaction [57], and are therefore difficult to detect directly. However, such neutrinos would be captured in the Sun by scattering from hydrogen therein and their pair annihilations in the Sun would produce energetic neutrinos from the Sun [57]. The results from searches for energetic neutrinos at e.g., Kamiokande have also ruled out Majorana neutrinos with mass less than a few hundred GeV [57].

2.2.5 Axions

Axion a is also one of the leading candidates for CDM. Axions were introduced by Peccei and Quinn [58] to solve the strong CP (charge-conjugation and parity) violation problem of QCD. They are pseudo Nambu-Goldstone bosons associated with the spontaneous breaking of a new global Peccei-Quinn (PQ) U(1) symmetry at scale f_a [55].

The present relic density of the axions can be given as [55]:

$$\Omega_a = k_a(\frac{f_a}{10^{12}GeV})^{1.175}\theta_a^2, \tag{2.14}$$

where f_a is the Axion decay constant, k_a is a numerical factor lying roughly between 0.5 and a few and θ_a is a misalignment angle which parameterizes the axion field. Suppose $\theta_a \approx 1$, axions will have the required cosmological energy density to be Dark Matter, if $f_a \approx 10^{11} GeV$. It is pretty comfortably above the laboratory and astrophysical constraints and this would correspond to an axion mass $m_a \approx 10^{-4} eV$[55].

Axions could be detected by looking for their conversion to microwave photons, $a \rightarrow \gamma$, in a strong magnetic field [55]. Such a conversion could proceed through the loop-induced $a\gamma\gamma$ coupling, whose strength $g_{a\gamma\gamma}$ is thus an important parameter of axion models [55]. Moreover, the conversion rate can be enhanced in a high quality cavity on resonance and, due to the equation $m_a c^2 = \hbar\omega_{res}$, varying this resonance frequency can give a range of m_a, or, equivalently, f_a [55].

2.2.6 Other possible SUSY candidates

Besides the Neutralinos and the sneutrinos, some other supersymmetric particles are also (theoretically) possible to be candidates for Dark Matter.

Axino is the spin–1/2 superpartner of the axion. It may be the LSP or the next-lightest supersymmetric particle (NLSP) and may decay to the LSP [57]. When the axino is the lightest supersymmetric particle and has a mass of a few keV, it can be a good candidate for Warm Dark Matter (WDM)[57].

Gravitino, the spin–3/2 superpartner of graviton, is also a possible candidate for Dark Matter. The gravitinos will decouple at temperatures of order of the Planck scale ($E_{Pl} \approx 10^{19} GeV$) [57]. Thus the physics of the gravitinos must be considered at energies and temperatures right up to this scale [57]. In addition, if gravitinos behave as standard stable thermal relics with an abundance determined by consideration of their decoupling, the mass of gravitinos should be less than a few keV [57]. However, in some models with gravitinos as LSP, the NLSP should decay to a gravitino plus ordinary particles [57]. Since the coupling to gravitinos is so weak, this NLSP will be very long-lived and the products of its decay will contain γ-ray with high energies [57].

2.3 Hot Dark Matter (HDM)

Hot has been used here to indicate that such Dark Matter particles moved relativistically in the early Universe. Due to their fast velocities, they would cover great distances and then form some very large scale structures. This means that the Hot Dark Matter forms the structure of our Universe from the top down, with super clusters fragmenting into clusters and galaxies [59]. It is in contrast to the observational evidence which indicates that the structure of our Universe has been formed from the bottom up by merging dust to galactic scale structures [59].

However, there are still some suggestions in which part of Dark Matter is hot and the rest is cold. In these models the bulk of the Dark Matter (especially in galactic halos) is still cold.

2.3.1 Massive neutrinos

The leading candidates for Hot Dark Matter are the massive neutrinos, WMAP results combined with other astronomical measurements lead to a contribution for light (but massive) neutrino species[55]:

$$\Omega_\nu < 0.014 \tag{2.15}$$

They could include the electron, muon, and tauon-neutrinos in the Standard Model with non-zero masses as well as the forth-generation Dirac and Majorana neutrinos with extremely light masses.

2.4 Dark baryons

As mentioned above, some CDM particles, e.g., neutralinos and axions, could form galactic scale structures such as galaxies and clusters of galaxies, while, some HDM particles, e.g., massive neutrinos, could form larger structures of the Universe. This means that on different scales Dark Matter might consist of different materials [57].

Moreover, in this chapter we presented some theoretically predicted (SUSY) particles as candidates for Dark Matter. However, until now there is no direct accelerator evidence for the existence of supersymmetry [57]. Actually, it is not absolutely certain that Dark Matter is neither baryons nor neutrinos [57]. There are also some conservative

cosmological models which describe the Universe only in terms of baryons and perhaps neutrinos [57].

On the other hand, the baryonic matter density in the Universe is

$$\Omega_b \approx 0.042 \tag{2.16}$$

but only around 25% of the baryonic matter is luminous:

$$\Omega_{lum} \approx 0.01 \tag{2.17}$$

Although, most of the baryons in the clusters of galaxies reside not in the galaxies themselves, but in form of hot intercluster, x-ray emitting gas [59], such hot gas in the clusters of galaxies only accounts for around 10% of the baryons in the Universe [59]. Hence, there should (must) be some baryonic Dark Matter.

Two most promising possibilities for such dark baryons are diffuse hot gas and dark stars, which include white dwarfs, neutron stars, black holes, or objects with masses around or below the hydrogen-burning limit [59].

2.4.1 Massive Astrophysical Compact Halo Objects (MACHOs)

Massive astrophysical compact halo objects include, for example, brown dwarfs which are balls of hydrogen and helium with masses $< 0.08M_{\odot}$ and therefore never begin nuclear fusion of hydrogen [57] (but they do burn deuterium), jupiters which are similar to brown dwarfs but have masses $\sim 0.001M_{\odot}$ [57] and do not burn anything, and white dwarfs [57]. Actually, objects with masses around or below the hydrogen-burning limit could be baryonic Dark Matter [59].

Further, neutron stars and stellar black-hole remnants are also candidates for baryonic Dark Matter [57]. Black holes with masses $\sim 100M_{\odot}$ could be remnants of an early generation of stars which were massive enough so that not many heavy elements were dispersed when they underwent their supernova explosions [57]. Primordial black holes which formed before the era of Big Bang could be counted for non-baryonic Dark Matter rather than baryonic one [55]. However, such an early creation of a large number of black holes is possible only in certain somewhat contrived cosmological models [55]. A brief description of the potential MACHO candidates is given below:

- **Brown Dwarfs**:
  Brown dwarfs are made out of hydrogen, the same as our sun but they are typically much smaller. Stars like our sun form when a mass of hydrogen collapses under its own gravity and the intense pressure initiates a nuclear reaction, emitting light and energy. Brown dwarfs are different from normal stars. Because of their relatively low mass, brown dwarfs do not have enough gravity to start hydrogen burning in their cores [41]. Thus, a brown dwarf is not a real star; it is an accumulation of hydrogen gas held together by gravity. Brown dwarfs give off some heat and a small amount of light [41].

- **White Dwarfs:**
  White dwarfs are products of final evolutionary stage of intermediate massive and low mass stars. They have two distinct features when compared to normal stars. First, they have a small radius ($\sim 10^{-2} R_{\odot}$) and high density ($10^2 gcm^{-3}$) and strong surface gravitational acceleration. Second their interiors do not have thermonuclear burning so their evolution rely on the dissipation of their own thermal energy. The Chandershaker limit for the mass of white dwarf is $\approx 1.4 M_{\odot}$ [42].

- **Neutron Stars:**
  If the initial mass of the star on the main sequence was not too large ($M \leq 25 M_{\odot}$), the remanent in the inner core will stabilize and become neutron star. The neutron stars are supported by degenerate neutron pressure. Their size is very small ($10km$) and have very large density. Similar to white dwarfs, neutron stars do not have thermonuclear reactions and their energy source in maintaining the external radiation is the dissipation of their internal heat energy [42].

- **Black Holes:**
  Black holes, unlike brown dwarfs, have an over-abundance of matter. All that matter collapses under its own enormous gravity into a relatively small area. The black hole is so dense that anything that comes too close to it, even light, cannot escape the pull of its gravitational field. Stars at safe distance will circle around the black hole, much like the motion of the planets around the sun . Black holes emit no light; they are truly black [42].

MACHOs might represent a large part of the galactic Dark Matter and could be detected through the microlensing effect [55]. The MACHO, EROS, OGLE collaborations

have performed programs of observation of such objects by monitoring the luminosity of millions of stars in the Large and Small Magellanic Clouds [55]. They concluded that MACHOs contribute $\leq 40\%$ (MACHO) or even $\leq 20\%$ (EROS) to the mass of the galactic halo [55]. Thus, MACHOs appear to be less likely candidates of dark matter implying that most Dark matter cannot exist in the form of baryonic astrophysical objects.

Chapter 3

Distribution Of Dark Matter

The existence of Dark matter in the universe, for which there is ample evidence now, automatically generates many other questions. For example: What is the nature of Dark matter? And how is it distributed in the universe? The first question has been discussed in chapter 2, even though the nature of dark matter is still unknown. In this chapter, we shall attempt to answer the second question i.e. the distribution of Dark matter in the universe.

The distribution of dark matter in the universe is being studied in a variety of ways: (a) by studying the large-scale distribution of galaxies, as with the Sloan Digital Sky Survey (SDSS); (b) by constraining the dark matter mass power spectrum through weak lensing studies, as by a future Large Synoptic Survey Telescope (LSST) and the Joint Dark Energy Mission (JDEM); and (c) by cataloguing massive clusters of galaxies as a function of redshift, using the Sunyaev-Zeldovitch effect, by the South Polar Telescope and the Atacama Cosmology Telescope. It is become increasingly evident that the distribution of dark matter is far from uniform. A larger portion may reside in the galaxy halos and even larger part in cluster cores. Large but uncertain content of dark matter has been reported in the local group. There are possibilities that galaxies exist in which there are so few stars that the galaxy is almost completely dark matter. However, there exist a modest number of objects and systems (e.g. open and globular star clusters) were little or no dark matter is present. These estimates are summarized in [60]. The distribution of luminous and dark matter in galaxies shows amazing properties and remarkable systematics that are bound to play a decisive role in discovering the nature of 'Dark Matter Phenomenon' and in building a successful theory of Galaxy Formation.

We begin our discussion with an account of the Distribution of Dark matter in galax-

ies. We will then explore the possibilities of presence of Dark matter in clusters and super clusters of galaxies.

3.1 Dark matter in galaxies

Galaxies are the most common objects in the universe. They are large systems of stars, gas and mysterious Dark matter. In 1929 Hubble classified the galaxies in to several types according to their overall observed shapes. According to this scheme Galaxies are distributed in to three (Regular) classes: Elliptical, Spiral and Bared spirals. The Irregular galaxies form a fourth class of objects in his system of classification. It appears that there are different amounts of dark matter in different types of galaxies. The description of Dark matter in different galaxies is described below:

3.1.1 Dark matter in spiral galaxies

The spiral galaxies are the most dominant galaxies in the universe. They account for about 77% of the observed galaxies. Our own galaxy, the milky way, is a typical spiral galaxy. The various parts of spiral galaxies are: nucleus, disk, halo and spiral arms. The spiral arms contain interstellar matter and young stars, whears the nucleus and the halo contain population-II stars (old stars). The spiral galaxies exist in a wide variety of forms. An artists impression of the predicted dark matter distribution (shown in blue) around the Milky Way (a typical spiral galaxy) is shown in figure 3.1:

Most of the luminous matter in spiral galaxies is concentrated in two components: a spheroidal bulge in which the projected density distribution is approximately described by

$$I(R) = I_0 e^{-7.67(\frac{R}{R_e})^{\frac{1}{4}}} \tag{3.1}$$

where R_e is the half-light radius.
And an extended disk with surface luminosity distribution [61]:

$$I(R) = I_0 e^{\frac{-R}{R_D}} \tag{3.2}$$

where R_D is the disk scale-length, I_0 is the mean value.

Since most of the matter in the Universe is invisible but most likely gravitating, we

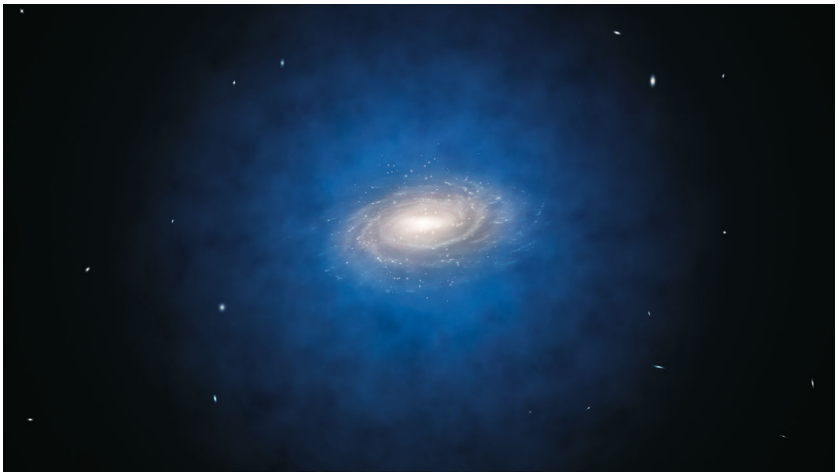

Figure 3.1: Dark matter distribution (shown in blue) around the Milky Way (Image Credit: L. Calada/ESO)

use Newton's Gravity to estimate the mass of the galaxy:

$$M(R) = \frac{V_{rot}^2 R}{G} \tag{3.3}$$

where V_{rot} is the rotational speed and G is a the universal gravitational constant. The total rotational velocity of the spiral galaxy is given by the velocity of the gas, stars, bulge and halo:

$$V_{total} = [V_{gas}^2 + V_{disk}^2 + V_{bulge}^2 + V_{halo}^2]^{\frac{1}{2}} \tag{3.4}$$

For the spherically symmetric halo velocity is $V_{halo}^2 = GM(R)/R$. The contributions to V_{total} from the bulge, stellar disk and gas disk are insufficient to give the observed V_{total}. Therefore, we require dark matter.

Disk structure

The rotation curves of spiral galaxies are flat and they go against the behaviour of planets inside the solar system. This flatness of rotation curves indicates the presence of non luminous matter in large quantities inside the spiral galaxies.

Persic, Salucci & Stel [62] and Salucci & Persic [63] while analysing a large number of rotation curves of spiral galaxies, found the existence of the universal rotation curve (URC). It means that, for every galaxy there exists its own profile of the rotation curve (see Fig 3.2). From the rotation curves of spiral galaxies the total velocity can be expressed as

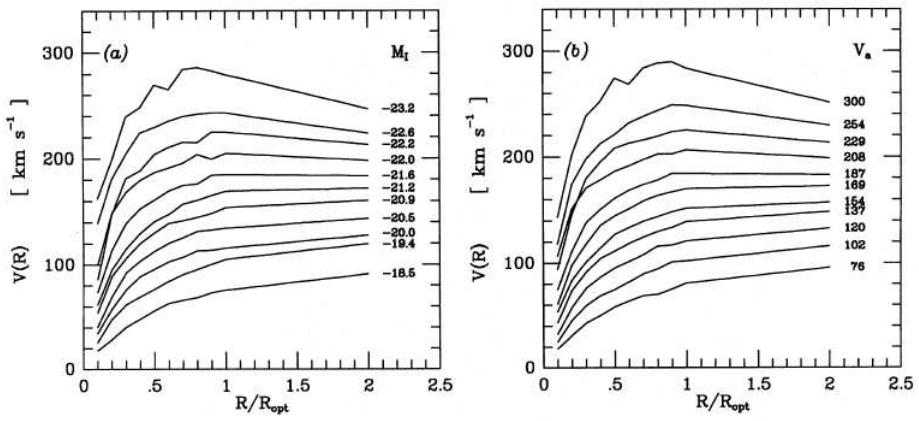

Figure 3.2: The universal rotation curve of spiral galaxies. Radii are in units of R_{opt} [64].

:

$$V = (V_{halo}^2 + V_{disk}^2)^{\frac{1}{2}} \tag{3.5}$$

where the square of disk velocity V_{disk}^2 is:

$$V_{disk}^2 = V^2(R_{opt})\beta \frac{1.97x^{1.22}}{(x^2 + 0.78^2)^{1.43}} \tag{3.6}$$

and the square of halo velocity V_{halo}^2 is given by :

$$V_{halo}^2 = V^2(R_{opt})(1-\beta)(1+\alpha^2)\frac{x^2}{x^2+\alpha} \tag{3.7}$$

where the value of variable x is expressed in the units of R_{opt} as :

$$x = \frac{R}{R_{opt}} \tag{3.8}$$

The Universal Rotation Curve (URC) fits of the combined contribution from the disk and

the halo would involve minimum errors (with in 1%) if we define the parameters α and β as:

$$\beta = 0.72 + 0.44\log(\frac{L}{L_*}) \tag{3.9}$$

$$\alpha = 1.5(\frac{L}{L_*})^{\frac{1}{5}} \tag{3.10}$$

where $L_* = 10^{10.4}L_\odot$. It is clear that if $L = L_*$ for a particular galaxy then α corresponds to a value of x of the order of R_{opt}, exactly $1.5R_{opt}$. Then the mass of a spherically symmetric halo can be expressed as :

$$M_{halo} = G^{-1}V^2R_{opt}(1-\beta)(1+\alpha^2)\frac{x^2}{x^2+\alpha} \tag{3.11}$$

and its density can be expressed as :

$$\rho = \frac{1}{4\pi R^2}\frac{dM}{dR} \propto \frac{x^2+3a^2}{(x^2+a^2)^2} \tag{3.12}$$

The Salucci & Persic [63] calculated the total mass of the halo by extrapolating the halo up to the radius of R_{200}. The estimated value of mass and radius of the halo are given as:

$$R_{200} = 250(\frac{L}{L_*})^{0.2}kpc \tag{3.13}$$

and

$$M_{200} \sim 2\times 10^{12}(\frac{L}{L_*})^{0.5}M_\odot \tag{3.14}$$

The mass luminosity ratio's of brighter galaxies were described as:

$$\frac{M_{200}}{L_B} \simeq 75(\frac{L}{L_*})^{-0.5} \tag{3.15}$$

The mass luminosity ratio's of brighter galaxies are very small as compared to that of faint galaxies. Therefore faint galaxies are rich in dark matter. The luminous to dark matter ratio's of brighter galaxies can be be expressed as:

$$\frac{M_{lum}}{M_{200}} = 0.05(\frac{L}{L_*})^{0.8} \tag{3.16}$$

For brighter galaxies the ratio $M_{lum}/M_{dark} \sim 1$.

The structure and density profiles of halo's show very small variation for different spirals on the scales of $(0.2-1)R_{200}$. However at very small radii, the profiles look totally different from each other, the core radius decreases with the decrease in M_{200} as:

$$\frac{R_{core}}{R_{200}} = 0.075(\frac{M_{200}}{10^{12}M_{\odot}})^{0.6} \tag{3.17}$$

The central density varies with the mass as:

$$\rho_{halo}(0) = 6.3 \times 10^{4}\rho_{c}(\frac{M_{200}}{10^{12}M_{\odot}})^{-1.3} \tag{3.18}$$

where $\rho_c = \frac{3H_o^2}{8\pi G}$ is the critical density of the Universe.

From the above discussion it is clear that the core radii of brighter galaxies are large and their central halo densities are small. Therefore the central regions of brighter galaxies are filled with the visible matter, while faint galaxies have their internal regions dominated by the dark matter.

Halo structure

The shapes of rotation curves have a direct impact on the structure of halos in spiral galaxies as predicted by the Cold Dark Matter (CDM) models. If we assume that the shapes of halos are spherical then the density profiles can be described as:

$$\rho(R) = \frac{\rho_0}{1 + (\frac{R}{R_c})^2} \tag{3.19}$$

where ρ_0 the central density and R_c the core radius.
The circular velocity is defined as:

$$V^2(R) = \frac{GM(R)}{R} \tag{3.20}$$

where $M(R)$ is the mass in a sphere of radius R. The circular velocity can also be expressed as:

$$V^2(R) = 4\pi G\rho_0 R_c^2[1 - \frac{R}{R_c}\arctan\frac{R}{R_c}] \tag{3.21}$$

which is an increasing function of R and attains a value $V_{max} = V(R = \infty)$, where

$$V_{max} = \sqrt{4\pi G \rho_o R_c^2} \tag{3.22}$$

The results of CDM (Cold Dark Matter) models suggest that the halos should be described by the NFW (Navarro, Frank and White)[65] profiles:

$$\frac{\rho(R)}{\rho_{crit}} = \frac{\delta_c}{\frac{R}{R_s}(1 + \frac{R}{R_s})^2} \tag{3.23}$$

where R_s is a scale radius, δ_c is a characteristic (dimensionless) density, and ρ_{crit} is the density of the critical Einstein-de Sitter Universe $\rho_{crit} = 3H_o^2/8\pi G$.

The Navarro, Frank and White (NFW) profile is also known as universal profile because it explains the rotation curves of most of the galaxies and clusters of galaxies. For the NFW halo the circular velocity can be extracted from:

$$(\frac{V_c(R)}{V_{200}})^2 = \frac{1}{x}\frac{\ln(1 + cx) - \frac{cx}{1+cx}}{c\ln(1 + cx) - \frac{c}{1+cx}} \tag{3.24}$$

where V_{200} is the circular velocity at R_{200} (virial radius) and the average value of ρ at $R = R_{200}$ is $< \rho >= 200\rho_{crit}$. The parameters c (called the concentration) and x are defined as $c = R_{200}/R_s$, $x = R/R_{200}$ respectively.
We can also express M_{200} by

$$M_{200} = (200\rho_{crit})\frac{4}{3}\pi R_{200}^3 = 100\frac{H^2}{G}R_{200}^3 \tag{3.25}$$

or

$$M_{200} \propto R_{200}^3 \propto V_{200}^2 \tag{3.26}$$

It is clear from the above discussion that, NFW density profiles involve two correlated parameters V_{200} and c, the halo density is proportional to the true density at the time of halo formation. Initially the halo density was very high but due to the hierarchical halo formation the functions $\rho_c(t)$ and $M_{200}(t)$ became decreasing functions. Therefore the galactic rotation curves are now one parametric.

The analysis of the dwarf spiral galaxies by Burkert [66] suggest that these galaxies

have similar density profiles. The observed universal mass profiles can be fitted as:

$$\rho_{DM}(R) = \frac{\rho_0 R_0^3}{(R + R_0)(R^2 + R_0^2)} \tag{3.27}$$

where ρ_0 and R_0 are free parameters which represent the central density and a scale radius, respectively. From the above expression we conclude that, for $R << R_o$ we have a finite central density ρ_o and the profile resembles with isothermal profile. While as for large radii the mass distribution diverges with increasing R. Thus Burkert profile completely agrees with the NFW profile.

The NFW profile is followed by most of the galaxies but some exceptions to this have been repoarted by Moore et al. [67]. They found a different model as best fit for the density profiles of high resolution halo. The model predicted and worked out by Moore et al. is given by

$$\rho(R) = \frac{\rho_0}{[(\frac{R}{R_s})^{1.5}(1 + (\frac{R}{R_s})^{1.5})]} \tag{3.28}$$

where R_s is a scale radius. This profile has a steeper asymptotic slope $\rho(R) \propto R^{-1.5}$. The computer simulations carried out by Fukushige & Makino [68] on 12 halos whose masses are in the range of $6.6 \times 10^{11} - 8 \times 10^{14M} M_{\odot}$, show a good agreement with the Moore et al. profiles.

They N-body simulations carried out by Hayashi et al. [69] does not agree with both NFW profile and profiles predicted by Moore et al. Thus the choice of the most efficient model would depend on the agreement between the theory and observation. However, among all the models NFW is the most consistant one.

3.1.2 Dark matter in Elliptical galaxies

Elliptical galaxies as their name suggests, have an elliptical appearence. The ellipticals are classified according to their degree of eccentricity. The elliptical galaxies contain mostly population-II (old) stars. They have much greater ranges in size and mass as compared to the spirals. Their masses cover a range: from about 10^7 up to $10^{13} M_{\odot}$. The corresponding range of diameters is about $1/10$ kpc up to about 100 kpc. In clusters of galaxies nearly 80% are ellipticals but they form only $20 - -25\%$ of the field galaxies. The large concentration of ellipticals in clusters of galaxies can some times mislead the studies. It is possible that the dark matter halos can be stripped away by gravitational

tidal force and added to other galaxies. Therefore, it is extremely difficult to estimate the amount of dark matter which the galaxy was having, and how much it has lost to the surrounding objects.

To estimate the mass of an elliptical galaxy, we employ several methods. Some of them are enlisted below:

- From the stellar velocity dispersion
- From the neutral gas velocities found in the outermost region, in some galaxies.
- From the X-ray corona surrounding ellipticals.
- Using gravitational lensing method.

According to de Vaucouleur's law [70] , the surface brightness of an ellipyical galaxy can be expressed as:

$$I(R) = I_e e^{-7.67((\frac{R}{R_e})^{\frac{1}{4}}-1)} \tag{3.29}$$

where R_e is the radius enclosing half of the light.

The velocity dispersions of stars calculated from the observations, when used in the virial theorem or Jeans equation can give the tatal mass for $R < R_e$ and other cases. When we employ the virial theorem for a spherical, steady state and static isothermal elliptical galaxy the result is:

$$2R = \frac{GM}{\sigma^2} \tag{3.30}$$

where R is a radius and σ^2 a velocity dispersion. The larger the mass, the larger the stellar velocities must be. From This formula we can estimate the mass.

In practice much more sophisticated models than this one are used to interpret the velocity dispersions.

There is no clear evidence which could suggest the uniform distribution of dark matter in elliptical galaxies. Carollo et al. [71], while examining the velocity dispersions of four elliptical galaxies concluded that, there is considerable amount of dark matter in three galaxies out of the four observed. De Paolis , Ingrosso and Strafella [72], found that there is negligible amount of dark matter with in the radius of R_e . In contrast to these, Bertin et al. [73], found that dark matter in elliptical galaxies is of the order of visible matter.

A small fraction of elliptical galaxies are surrounded by a ring of neutral hydrogen, in these cases, the determination of a dark matter halo is very similar to its determination in spiral galaxies, from the rotation curve. Schweizer, van Gorkom & Seitzer [74] found evidence for a DM halo in IC 2006 with twice the mass of the luminous matter within $6.5R_e$, under the assumption that the HI ring is flat and circular. Bertola et al. [75] analyzed five elliptical galaxies, combining the M/L ratios obtained with the inner ionized hydrogen component and the outer neutral hydrogen ring. M/L is constant out to about $R_e \sim 3.5 \pm 0.9$ but becomes very large in the ring region.

The analysis of the hot X-ray emissions from the galactic halos is one of the important methods to study dark matter in elliptical galaxies. The hot X-ray emissions extends to the scales of $50kpc$ [76]. The typical mass of this hot gas is about $10^{10}M_{\odot}$ and it originates from the matter lost from the stars. Therefore, for a spherical dark matter halo, if this gas is assumed to be in hydrostatic equillibrium we can calculate the mass as:

$$M(R) = \frac{kTR}{Gm}\left[\frac{d\ln\rho}{d\ln R} + \frac{d\ln T}{d\ln R}\right] \tag{3.31}$$

where ρ is the density of the gas. The temperature profile $T(R)$ provided by the observations usually involves lot of errors, Inspite of this if $M(R)$ is known, we can obtain the dark matter halo profile.

O'Sullivan & Ponman [77] analysed a Chandra observation of the elliptical galaxy NGC 4555. They found that NGC 4555 has a large gaseous halo, extending to $\sim 60kpc$. The gas temperature is $0.95keV$ and the Iron abundance to be $\sim 0.5Z_{\odot}$. Authors model the surface brightness, temperature and abundance distribution of the halo and used these results to estimate parameters such as the entropy and cooling time of the gas, and the total gravitational mass of the galaxy. The results show that NGC 4555 has a massive dark halo and large mass-to-light ratio ($56.8M_{\odot}/L_{B\odot}$ at $50kpc$).

The image splitting of an individual gravitational lens system consisting of an elliptical is only slightly sensitive to the existence of a DM halo, and so, one cannot definitely discriminate between galaxies with and without halos, with some exceptions [78, 79]. In three cases where the lens is clearly a single galaxy, there is no need to consider any dark matter halo.

Globular clusters have been considered to deduce the existence of dark matter halos in ellipticals, mainly in $M87$. Mould et al. [80] support the conclusions obtained by other

methods: models without dark halos do not fit the data in $M87$.

From the above discussion we conclude that, there are some evidences which support the existence of dark matter in elliptical galaxies, but these evidences are not as clear as we have in spiral galaxies.

3.1.3 Dark matter in dwarf spheroidal galaxies

The Dwarf Speroidal (DSph) galaxies are the low luminosity galaxies and are believed to be the most dominant in the universe. Dwarf galaxies are composed of up to 99 percent dark matter and only one percent normal matter like stars. This disparity makes dwarf galaxies ideal targets for astronomers seeking to understand dark matter. However, Dwarf spheroidal (DSph) do not have gas in the periphery and the determination of dark matter is more problematic. There are two methods for detecting DM in dwarf spheroidals:

First one is the comparision of the virial mass with the luminous mass of these galaxies. The relation between the luminosity and mass of these galaxies estimated by Salucci & Persic [63], is $M \sim L^{\frac{1}{4}}$. The M/L ratio's calculated by Mateo et al. [81] , is of the order of 100. If we assume that, the spatial distribution of luminous dark matter is same inside the galaxy then we can use the virial theorem to calculate the central density ρ_o as:

$$\rho_o = \frac{9\sigma_0^2}{4\pi G R_c^2} \tag{3.32}$$

where ρ_0 is the central density,σ_0 the central velocity dispersion and R_c a core radius. Within this radius the mass is $\rho_0 \frac{4}{3}\pi R_c^3$ and the luminosity is $\Sigma_o \pi R_c^2$, where Σ_o is the observable central surface brightness. The M/L ratio would be

$$\frac{M}{L} = \frac{3\sigma_o^2}{\pi G \Sigma_o R_c} \tag{3.33}$$

Since the velocity dispersions of these galaxies are small ~ 10 km/s therefore, we require high spectral resolution.

The second method is to use the tidal radii. The dwarf spheroidal galaxy considered as the satellite of a primary galaxy (like Milky Way), could become tidally disrupted if it does not have enough dark matter. And thus increasing selfgravitation and preventing it. The radius of the satellite necessary for selfgravitation to match tidal disruption is

determined by the formula:

$$r = R\left(\frac{m}{M}\right)^{\frac{1}{3}}, \tag{3.34}$$

where r is the radius of dwarf galaxy and m its mass, R is the distance between two galaxies and M is a mass of primary galaxy. At a galacto-centric radius equal to the critical value, r, stars would escape and would be trapped in the gravitational field of the primary galaxy. Thus at a tidal radius, r, the density should drop to zero. From the observational standpoint, the tidal radius is not so easy to define. It is typically measured from the photometric profiles and fits to King-like models. However, tides are likely to elongate systems and cause the velocity distribution to become more radial near the tidal limits of the system [82].

Recent measurements contradict a basic prediction about the structure of cold dark matter in dwarf galaxies. While computer simulations show that dark matter should be densely packed in the centers of galaxies, these new measurements of two dwarf galaxies (figure 3.3) show that they contain a smooth distribution of dark matter. This contradicts simulations using the standard cosmological model known as lambda-CDM.

3.1.4 Dark matter in Irregular galaxies

The galaxies which lack both a dominant nucleus and rotational symmetry are Irregular galaxies (Irr's). The mass of these galaxies lies in the range of $10^8 - 10^{10} M_\odot$ and their size varries from 1kpc to 10kpc. The Irregular galaxies have a large gaseous component. Using HI and optical observations of these galaxies one can measure the rotational velocities of these galaxies (like for normal spirals). Usually Irr's have a well defined rotation curves. The maximum rotational velocity is of the order $\sim 60 kms^{-1}$. The rotation curve rise slowly to the last measured point. Because of the large gaseous component this type of galaxies gives a possibility to measure the velocity to larger radius, with respect to spirals. Also the absence of the bulge makes analyses simpler. The rising rotation curves implies an existence of essential dark matter halo.

The existence of Universal Rotation Curve (URC) for the irregular galaxies was established by Salucci and Persic [63, 83]. With the coefficients α and β described as:

$$\alpha = 0.93 \times (\frac{V_{opt}}{63 kms^{-1}})^{-0.5}, \tag{3.35}$$

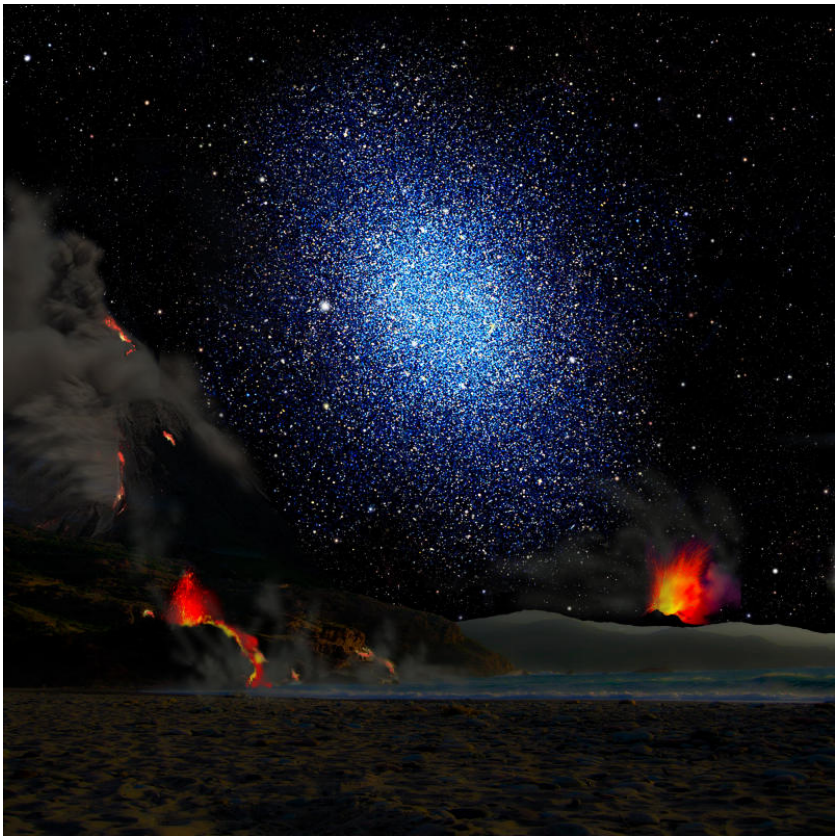

Figure 3.3: Artist's conception of a dwarf galaxy seen from the surface of a hypothetical exoplanet. The dark matter in dwarf galaxies is distributed smoothly rather than being clumped at their centers. (Figure Credit: David A. Aguilar (CfA))

and

$$\beta = 0.08 \times (\frac{V_{opt}}{63kms^{-1}})^{1.2} \tag{3.36}$$

The Irregular galaxies are very rich in dark matter thus, they make a good contribution to the total amount of baryonic dark matter in the universe.

3.2 Formation History Of Galaxies

Galaxies are born out of primordial fluctuations with an evolution probably driven by gravitation as the dominant effect. The models of galaxy formation have in common the hypothesis that the dark matter is cold (CDM) and that, at a given time, CDM halos arose through a hierarchy of different sized halos formed from mergers of smaller halos. At least four steps characterize the evolution of a galaxy:

- Small density fluctuations, probably originated by quantum fluctuations before the epoch of Inflation or at cosmological phase transitions, grow during the radiation dominated Universe and provide a fluctuation spectrum after the epoch of Recombination.

- CDM overdensities accrete matter and merge. The hierarchical formation of greater and greater halos produces the present galactic and cluster structures.

- Baryons cool and concentrate at the centre of halos and constitute the visible component of galaxies. The explanation of the Hubble sequence and the origin of rotation of galaxies would be goals of the study of this phase.

- Once the basic structure of a galaxy with its different components has been established, it is necessary to follow its evolution due to star formation, gas ejected from stars, progressive metal enrichment, matter flows connecting the intra and extra media, small internal motions.

Dalcanton et al. [84] proposed the following model of the disk formation:

- The tidal torquing spins up both dark matter and the baryonic matter in some region of space. Assuming that gas and dark matter are uniformly mixed.

- As the time passes, both the dark and baryonic matter begin to collapse in the overdense region. Initially, when the densities are low, the baryons cannot cool, and the pressureless collapse proceeds identically for both components.

- Because the dark matter cannot dissipate energy, its collapse halts when the system virializes.

- The authors approximate the halo with Hernquist density profile, with asymptotic radial profile scales as R^{-4}.

$$M_{halo}(R) = (1 - F)M_{\infty}(\frac{R/R_0}{1 + R/R_o}) \tag{3.37}$$

where $M_{halo}(R)$ is the halo mass within radius R, R_0 a core radius, and F is the fraction of baryonic mass of the protogalaxy within some radius a.

The potential energy within a radius R is

$$\phi(x = 1 + \frac{R}{R_0}) = -\frac{(1-F)GM_\infty^2}{6R_0}(1 - \frac{6x^2 - 8x + 3}{x^4}) \tag{3.38}$$

The size of the core radius depends only on the mass of the halo and the mean density of the Universe.

- During the joint collapse of dark matter and baryons, at some point the density over some region becomes high enough that the baryons begin to cool and decouple from the dark matter. As they cool, their collapse accelerates, and the baryons begin to concentrate within the dark matter. This condensation increases the baryonic fraction within the inner parts of the halo. Since the baryons have nonzero angular momentum, they cannot collapse all the way to the center and instead settle into a rapidly rotating disk. The final mass distribution in the disk is determined both by the initial distribution of specific angular momentum and by the final rotation curve of the collapsed disk plus halo system.

- After the onset of cooling, the collapsing baryons further condense the dark matter halo by increasing the mass density in the inner parts of the halo, where the baryonic mass fraction has increased the most. This modifies the Hernquist potential which the halo had at the time when the cooling began. The condensation of the halo is assumed to proceed roughly adiabatically.

3.3 Dark matter in clusters of galaxies

The clustering of spiral nebulae was recognised long before their extragalactic nature was universally accepted [85], and a dynamical study of Virgo cluster[5], was among the first indicators of Dark matter in the universe. Nearly all modern studies concur with this pioneering one in finding cluster mass-to-light ratios considerably larger than those of individual galaxies, even ones with extensive rotation curves. Published M/L values range from 30 to 1000, but this narrows considerably when normalised to a single value of H_0, face-on galaxies, and a single waveband for L. Usually, we take $M/L(H = 50) = \frac{1}{2}M/L(H = 100)$, $M/L_V \approx 0.7M/L_B$ and probably $M/L_{bol} \approx \frac{1}{2}M/L_V$.

There is still another factor of two between the virial mass $(2T + U = 0)$ and the jest bound mass $(T + U = 0)$, and finally M/L drops by yet another factor two when

corrected for absorption in our galaxy and normalized to face-on external galaxies [86]. It is not always very easy to determine which set of parameters was used in a particular study, but virtually all the very large values found in the literature drop to $100 - 200$ for face-on galaxies, the correct choice of solar L_V, and $H = 50 kms^{-1} Mpc^{-1}$ [86].

Virial M/L values of 100 or more have been obtained for Virgo [87], Coma [88], Perseus [89] and a number of other rich clusters[90] including one at a redshift of 0.39 [91]. Estimates other than the virial theorem yield concordant, but typically slightly larger masses [92]. Some uncertainty attaches to these numbers owing to faint galaxies in the clusters which cannot be counted directly and are included using an average luminosity function[93]. Light from obvious galaxies or from their extreme outskirts is also rather poorly measured, but almost certainly less than that seen in the galaxies. M/L could be changed by a factor of $2 - 4$.

More uncertainty comes from cluster dynamics. If for instance M/L is not constant throughout Coma, acceptable fits to measured velocities can be achieved with masses from $6 \times 10^{14} M_\odot$ and circular orbits in the outskirts to $5 \times 10^{15} M_\odot$ and radial orbits far out [94],corresponding to $M/L_B = 40 \; to \; 300 (H_0 = 50)$. If outer parts of clusters are not relaxed, Virial theorem masses could be too large by factors of $3 - 5$. An extreme version of this idea associates Dark matter only with central dominant galaxies, the others acting like unrelaxed test particles. Finally some clusters are certain to be contaminated by foreground and background galaxies that will push up the velocity dispersion and so M/L or to contain substructures that can have the same effect. All these considerations serve primarily to widen the error bars on M/L,though perhaps more in the direction of low values than high ones.

Potential wells of rich clusters can also be probed via X-ray emission of hot gas in them. The standard assumptions of hydrostatic, isothermal gas lead to M/L values of 100 or more [95], with the usual noise coming from different choices of distance, luminosity scale, etc. Once this noise is eliminated, results from analyses that assume different gas distributions and temperature, structures are not terribly discordant, With $M/L \sim 200h$, although the X-ray gas itself contributes as much as 30% of the mass in this case.

It is believed that 100-kpc halos must have blended in cluster cores where the intergalactic distance is small. In addition ,halos attached to the individual galaxies would make them hefty enough to segregate, the most massive ones falling to the centre. While morphological segregation in clusters is conspicuous [96],luminosity segregation is much

less so leading to a majority conclusion that $M/L \leq 30$ for individual cluster galaxies [97]. A similar limit comes from the requirement that gravitational drag heating of X-ray gas should not to be so large as to prevent cooling flows where they are seen [98]. The amount of Dark matter in rich clusters could, however, easily be the same as would have been associated with the individual galaxies in a less dense environment [99]. The likelihood of this depends mostly on how you think galaxies formed, but in any case most of the Dark matter must now belong communally to the cluster, not individually to the galaxies.

In 2004, The Hubble Space Telescope discovered a "ring" of dark matter (Figure 3.4) in the galaxy cluster Cl 0024+17. The ring is one of the strongest pieces of evidence to date for the existence of dark matter. It is believed that the dark matter ring was produced from a collision between two gigantic clusters. Recently, NASA's Hubble Space Telescope spotted an overabundance of dark matter in the heart of the merging galaxy cluster Abell 520. Figure (3.5) shows two different results concerning the amount of dark matter in the core of the merging galaxy cluster Abell 520. In the top image observations of the cluster, taken by Douglas Clowe with the Advanced Camera for Surveys, mapped the amount of dark matter in Abell 520. It reveals an amount of dark matter astronomers expect based on the number of galaxies in the core. The dark-matter densities are marked in blue, and the dotted circle marks the dark-matter core. The map is superimposed onto visible-light images of the cluster. In the bottom image a second team, led by James Jee, used the Wide Field Planetary Camera 2 to find an unusual overabundance of dark matter in the clusters core, denoted by the bright blue color at image center. The observation was surprising because astronomers expect that dark matter and galaxies should be anchored together, even during a collision between galaxy clusters.

Figure 3.4: The Hubble Space Telescope image of the galaxy cluster Cl 0024+17. The ring of Dark Matter is clearly visible.

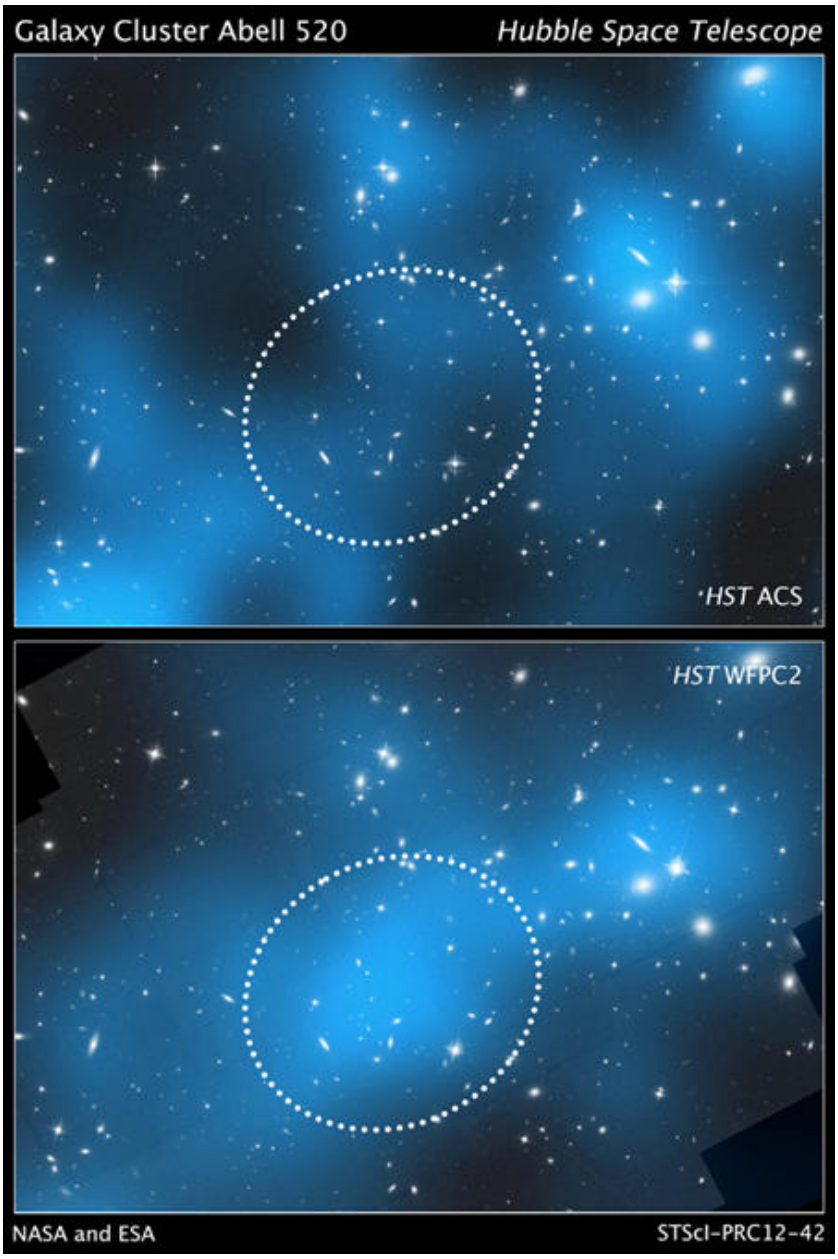

Figure 3.5: These composite images taken by two different teams using the Hubble Space Telescope show different results concerning the amount of dark matter in the core of the merging galaxy cluster Abell 520.(Figure Credit: J. Jee, University of California, Davis)

Chapter 4

Detection of Dark matter

4.1 Introduction

The baryonic Dark matter can be detected only through its gravitational interaction with the ordinary matter. Since baryonic Dark matter can not account for all the Dark matter in our universe so WIMPs (Weakly interacting massive particles) turn out to be the well motivated candidates. Despite persuasive indirect evidence for the existence of dark matter in the universe and in galaxies, the direct detection of dark matter remains one of the outstanding experimental challenges of present-day physics and cosmology.

The detection of Dark matter is very important to determine its properties and the role which it plays in the structure formation. Many experiments have searched and are currently searching for a signal of WIMP-like dark matter and each uses a different detection method. Although, producing dark matter in a particle accelerator would be ideal, but there are other methods as well which are also important for the detection of Dark matter.

In this chapter, we shall discuss both direct and indirect methods which are being employed for the detection of Dark matter. Although the process of detection of dark matter is still at the preliminary stage but we are expecting a breakthrough in near future as lot of experimentation is going on at present.

4.2 Direct Detection

The basic idea of direct detection is simple: set up a very sensitive device, containing a large amount of some element, which can detect very small motions and interactions of the atoms within it. If dark matter is everywhere in the Universe, then it should be traveling around (and through) the Earth, and therefore through a detection apparatus, at all times. It is an established fact that WIMPs would have annihilated to some ordinary matter, e.g., quarks and leptons, in the early Universe. Otherwise, they would have unacceptable large abundance today. According to the crossing symmetry, the amplitude for WIMP annihilation to, for example, quarks is related to the amplitude for elastic scattering of WIMPs from quarks [57]. Therefore, WIMPs should have some small, but non zero couplings to ordinary matter. Due to this coupling to nucleus (through the coupling to quarks), WIMPs could scatter elastically from target nuclei of the detector material and produce nuclear recoils which deposit energy in the detector. Hence, one of the most promising methods of detecting Galactic Dark Matter is the direct detection of WIMPs [100]. It is to be noted that, although the lightest neutralino is the leading candidate for Dark Matter, such WIMP direct searches are not specialized to detect the neutralino but any particle with similar generic properties, e.g., a mass between a few GeV and a few TeV and weakly interacting with ordinary matter [101].

4.2.1 Elastic WIMP-Nucleus Scattering

Using the standard assumption of the WIMP density near the Earth

$$\rho_0 \approx 0.3 GeV/c^2/cm^3 \tag{4.1}$$

and assuming a WIMP mass

$$m_\chi \approx 100 GeV/c^2, \tag{4.2}$$

the number density of WIMP can be found as

$$n = \frac{\rho_0}{m_\chi} \approx 3 \times 10^{-3} cm^{-3} \tag{4.3}$$

Meanwhile, by the assumption that the halo WIMPs are gravitationally bound to the Galaxy and its halo, the average velocity of WIMP wind is then approximately equal

to the stellar velocity in the Solar neighborhood:

$$\langle V \rangle \approx 250 km/s \tag{4.4}$$

Therefore, the WIMP flux is $\sim 10^5$ WIMPs per square centimeter of the Earth's surface per second.

However, the very low cross section of WIMPs on ordinary material makes the elastic WIMP-nucleus scattering very rare. In typical SUSY models with neutralino WIMPs, WIMP-nucleus cross section is about $10^{-6} - 10^{-4}$pico-barn $(10^{-42} - 10^{-40} cm^2)$ and the expected event rate is then at most 1 event/kg/day [55]. In some models, it is even less than 1 event/ton/yr [102]. With expected WIMP mass in the range $10 GeV/c^2$ to $10 TeV/c^2$ [55], typical nuclear recoil energies are of order of 1 to 100 keV. On the other hand, in the energy range from a few to a couple hundred keV, typical background noise due to cosmic rays and ambient radioactivity is much larger. Thus an underground laboratory and extensive shielding around the detector to protect against cosmic-ray induced backgrounds, and selection of extremely radio pure materials are necessary and important [55].

The event rate of elastic WIMP-nucleus scattering depends on various parameters coming from astrophysics, particle physics and nuclear physics: the WIMP density near the Solar system ρ_0, the WIMP-nucleus cross section, the WIMP mass m_χ, and the velocity distribution of the incident WIMPs $f(v)$ in the Galactic halo near the Earth. However it is seen that the expected event rate mainly depends on two unknowns: the mass of the incident WIMPs and the WIMP-nucleus cross section. Hence the experimental observable is usually expressed as a contour in the WIMP mass-cross section plane, although it is basically the scattering rate and is a function of energy [55].

Rate For Elastic WIMP-Nucleus Scattering

The direct detection experiment measures the number of events per unit time per unit mass of detector material as a function of the energy deposited in the detector Q. Qualitatively, the event rate of direct detection, R, can be simply expressed as [57]:

$$R \approx \frac{n \langle v \rangle \sigma}{m_N} \tag{4.5}$$

where $\langle v \rangle$ is the average velocity of the incident WIMPs relative to the earth frame (i.e., to the target), σ is the WIMP-nucleus cross section, and m_N is the mass of the target

nucleus. Here we multiply the factor $1/m_N$ to get the number of target nuclei per unit mass of the detector material.

More accurately, one should take into account the fact that the WIMPs move in the halo with velocities determined by their velocity distribution function $f(v)$, and that the differential cross section depends on $f(v)$ through an elastic nuclear form factor $F(q)$.

$$d\sigma = \frac{1}{v^2}(\frac{\sigma_0}{4m_r^2})F^2(q)dq^2 \tag{4.6}$$

Here σ_0 is the total cross section ignoring the form factor suppression,

$$m_r = \frac{m_\chi m_N}{m_\chi + m_N} \tag{4.7}$$

is the reduced mass, q is the transferred 3-momentum:

$$q = \sqrt{2m_N Q} \tag{4.8}$$

Therefore, in general, the differential scattering event rate (per unit detector mass) should be written as [57]:

$$dR = \frac{\rho_0}{m_\chi m_N}\int v f_1(v) d\sigma dv = (\frac{\rho_0 \sigma_0}{2m_\chi m_r^2})F^2(Q)\int \frac{f_1(v)}{v} dv dQ \tag{4.9}$$

where $f_1(v)$ is the one-dimensional velocity distribution function (Generally assumed to be Maxwell-Boltzmann distribution) of WIMPs impinging on the detector, v is the absolute value of the WIMP velocity in the Earth rest frame, and we have to integrate over all possible incoming velocities. By means of classical mechanics, the transferred momentum q can be expressed as:

$$q = 2[m_N(\frac{m_\chi v}{m_\chi + m_N})]\sin(\frac{\theta_{CM}}{2}) = 2m_r v\sqrt{\frac{1-\cos\theta_{CM}}{2}}, \tag{4.10}$$

where θ_{CM} is the scattering angle in the center-of-momentum frame. Since $0 \leq 1 - \cos\theta_{CM} \leq 2$, for a given deposited energy Q, we have

$$Q = \frac{(2m_r v_{min})^2}{2m_N} = \frac{2m_r^2 v_{min}^2}{m_N} \tag{4.11}$$

i.e., the minimal incoming velocity of incident WIMPs that can deposit the energy Q in

the detector can be expressed as

$$v_{min}(Q) = \sqrt{\frac{m_N}{2m_r^2}}\sqrt{Q} = \alpha\sqrt{Q}, \tag{4.12}$$

where

$$\alpha = \sqrt{\frac{m_N}{2m_r^2}}, \tag{4.13}$$

Then the differential event rate for elastic WIMP-nucleus scattering, Eq.(4.9), can be rewritten as

$$\frac{dR}{dQ} = A'F^2(Q)\int_{v_{min}}^{\infty}\frac{f_1(v)}{v}dv, \tag{4.14}$$

where the constant coefficient A' is defined as

$$A' = \frac{\rho_0\sigma_0}{2m_\chi m_r^2}. \tag{4.15}$$

It is to be noted that, first, α defined in Eq.(4.13) depends only on the WIMP mass m_χ and the mass of the target material, m_N, (which we can choose). There are still two unknown parameters, i.e., the WIMP density ρ_0 and the total WIMP-nucleus cross section σ_0, have been collected in the coefficient A' defined in Eq.(4.15). Second, we have assumed here that the detector essentially only consists of nuclei of a single isotope. If the detector contains several different nuclei (e.g., NaI), the right-hand side of Eq.(4.14) has to be replaced by a sum of terms, each term describing the contribution of one isotope. For simplicity, we will only focus on mono-isotopic detectors.

Finally, the total event rate per unit time per unit mass of detector material can be expressed as

$$R = \int_{Q_{th}}^{\infty}(\frac{dR}{dQ})dQ, \tag{4.16}$$

where Q_{th} is the threshold energy of the detector.

4.2.2 Target material dependence

The WIMP-nucleus cross section σ_0 in Eqs.(4.6) and (4.15) depends on the nature of the WIMP couplings to nucleons. For non-relativistic WIMPs, one in general has to distinguish spin-independent (SI) and spin-dependent (SD) couplings [55].

Spin-independent (SI) cross section

The total cross section for scalar coupling can be expressed as [57]:

$$\sigma_{0,scalar} = \frac{4m_r^2}{\pi}[Zf_p + (A-Z)f_n]^2 \tag{4.17}$$

Here m_r is the reduced mass of the WIMP and the target nucleus in Eq.(4.7), Z is the atomic number, $A-Z$ is then the number of neutrons, f_p and f_n are the effective couplings of WIMPs to protons and neutrons, respectively.

Here we have to sum over the couplings to each nucleon before squaring because the wavelength associated with the momentum transfer is comparable to or larger than the size of the nucleus [103], the so-called coherence effect. In most cases, the couplings to protons and neutrons are approximately equal [57],

$$f_n \simeq f_p \tag{4.18}$$

Then the cross section for scalar interaction in Eq.(4.17) can be reduced to

$$\sigma_{0,scalar} \propto A^2. \tag{4.19}$$

This means that, due to the coherence effect with the entire nucleus, the cross section for scalar interaction scales approximately as the square of the atomic mass of the target nucleus. Hence, higher mass nuclei, e.g., Ge or Xe, are preferred for the search for the scalar interaction [55]. On the other hand, WIMPs could also have a vector coupling to protons and neutrons [57]:

$$\sigma_{0,vector} = \frac{m_r^2}{64\pi}[2Zb_p + (A-Z)b_n]^2 \tag{4.20}$$

where b_p and b_n are the effective couplings to protons and neutrons. However, for Majorana WIMPs ($\chi = \bar{\chi}$), e.g., the neutralino, there is no such vector interaction [55].

Spin-dependent (SD) cross section

WIMPs could also couple to the spin of the target nucleus, an axial-vector (spin-spin) interaction. For this spin-spin coupling, only unpaired nucleons contribute significantly to the interaction, as the spins of the A nucleons in a nucleus are systematically anti-

aligned [103]. And it is obvious that this spin-dependent interaction exists only if the incident WIMPs carry spin [55].

The total cross section for spin coupling can be expressed as [57]:

$$\sigma_{0,axial} = \frac{32 m_r^2}{\pi}[\Lambda^2 J(J+1)], \tag{4.21}$$

where J is the total angular momentum of the nucleus and $\Lambda(\propto 1/J)$ depends on the axial couplings of WIMPs to the quarks.

Because of the dependence on the nuclear spin factor, the useful target nuclei for search for spin interaction are ^{19}F and ^{127}I [55].

Comparison of the SI and SD cross sections

Generally speaking, a WIMP could have both scalar and spin-dependent interactions with the nucleus. Thus the WIMP-nucleus cross section σ_0 in Eqs.(4.6) and (4.15) should be the sum of the scalar cross section, $\sigma_{0,scalar}$, in Eq.(4.17) and the spin cross section, $\sigma_{0,axial}$, in Eq.(4.21).

For the scalar interaction, an analytic nuclear form factor, e.g., the exponential form factor can be used. For the spin interaction, the form factor will differ from nucleus to nucleus and no simple analytic form factor can provide a very good approximation [57]. Fortunately, for nuclei with $A \geq 30$, the scalar interaction almost always dominates the spin interaction [57].

Target mass

The scattering event rate depends also on the atomic mass of the target material directly. First, according to Eq.(4.12), the smaller α the lower the incoming velocity with which the incident WIMPs can deposit energy larger than the threshold energy. Meanwhile, according to the definitions of α and m_r in Eqs.(4.13) and (4.7), it can be found that, for WIMPs with a given mass and detector with a given threshold energy, α will be smallest if the mass of the target nucleus m_N is equal to the WIMP mass m_χ. Second, for a given total mass of detector material, a larger target mass means also a smaller number density of the nucleus which can interact with the incident WIMPs. It will certainly reduce the total event number.

4.2.3 Measurement of recoil energy

There are various ways through which we can measure recoil energy, some of them we describe here:

A simple estimate

As an example, we assume a WIMP mass

$$m_\chi \approx 100 GeV/c^2, \tag{4.22}$$

and we use the standard theoretical WIMP rms velocity

$$\langle v^2 \rangle^{\frac{1}{2}} \simeq 270 km/s \tag{4.23}$$

then the average kinetic energy of the incident WIMPs can be estimated as

$$\langle E_\chi \rangle \approx 40 KeV. \tag{4.24}$$

On the other hand, by means of classical mechanics, the recoil energy of the target nucleus due to the elastic scattering can be expressed as

$$Q = [\frac{4 m_\chi m_N}{(m_\chi + m_N)^2} cos^2 \theta_{Lab}] E_\chi, \tag{4.25}$$

where θ_{Lab} is the recoil angle in the laboratory frame. This expression shows that the maximum recoil energy is obtained when $m_N = m_\chi$. This is also why this search should be more efficient for target material with a mass comparable to the WIMP mass.

Induced signals

When a WIMP scatters off a nucleus, the nucleus will at first obtain a few tens of keV kinetic energy and then dissipate this energy in the detector via three main processes: the electrons can be stripped by the scattered nucleus and an ionized nucleus-electrons system will be produced, this electronic activity can emit light, and the movement of the recoiling nucleus in the lattice can also induce vibrational phonons. Moreover, the ionization and scintillation energy will convert into phonons that will eventually thermalize and produce

a tiny elevation of the temperature in the detector.

Hence, generally speaking, due to the elastic WIMP-nucleus scattering, the nuclear recoil can induce three different signals: ionization (charges), scintillation (light), and heat (phonons).

Quenching factor

When a photon with energy between keV and MeV enters a detector, it will induce an electron recoil with a range of the order of the μm (10^{-6}m) and transfer most of its energy to the electron. However, the range of a nuclear recoil is only of the order of the nm (10^{-9}m) and the nucleus will lose a substantial part of its energy directly into phonons associated with atom vibrations as the nucleus is stopped in the lattice [103].

Hence, the quenching factor (the nuclear recoil relative efficiency) for the ionization detectors has been defined as the ratio of the number of charge carriers produced by a nuclear recoil due to the WIMP interaction to that produced by an electron recoil with the same kinetic energy (energy calibrated with a γ-source, called electron equivalent energy or eee). Meanwhile, for scintillating detectors, the quenching factor is defined as the ratio between the light produced by a nuclear recoil and by an electron recoil. For conventional detectors, this factor is usually lower than 0.3 [56], for Ge or Si, ~ 0.25 for Na, ~ 0.09 for I, and ~ 0.2 for Xe. While, for cryogenic detectors measuring heat, the quenching factor has been measured to be around one for recoiling nuclei independently of the energy [56].

It is to be noted that, due to this quenching factor, the measured recoil energies are often quoted practically in KeV_{ee} instead of true recoil energies in unit of KeV.

Heat

Basically a cryogenic detector is made of a crystal with a thermometer glued on it, and operated at very low temperature (around $20mK$). When the detectors have been cooled to the operating temperature in a dilution refrigerator, the heat capacity ($\propto T^3$) is so low that even a few keV of deposited energy raises the temperature of one of the detectors by a measurable amount, allowing the amount of energy deposited to be determined [57].

Moreover, a superconducting-normal phase transition due to the elevation of the temperature has been used by the CRESST collaboration [104]. A thin film of tungsten (W) can be grown on a silicon detector and held just below the critical temperature.

Phonons created by a WIMP-nucleus scattering would heat the superconducting film, causing it to go normal, and the change in resistance could be measured [57]. A very low threshold energy ($\simeq 500eV$) of such detector were reached by the CRESST-I experiment with a $262g$ sapphire detector [56].

Similarly, it is also possible to use some small superconducting granules in a magnetic field as detector, when one of such detectors is heated by a nuclear recoil, it would go normal and thereby cause a measurable change in the magnetic flux [57].

Ionization

A small voltage is placed across the crystal of the detector, and when several atoms have been ionized, the freed electrons will drift to one side, the collected charges can be used as a measure of the energy deposited in ionization [57].

Germanium ^{76}Ge used initially in the neutrino-less double-β ($0\nu2\beta$) decay experiments has been used as the first detector material for direct WIMP detection experiments by the Heidelberg-Moscow (HDMS) collaboration [105]. Thanks to the high intrinsic purity achieved by the semiconductor industries and the technique developed for the $0\nu2\beta$ decay experiments, Ge ionization detectors have nowadays very low thresholds and very good resolutions ($Q_{th} \simeq 4 \sim 10KeV_{ee}$, equivalent to $\simeq 15 \sim 30keV$ recoil energy, for HDMS [56]). Moreover, silicon (Si) has also been used by e.g., CDMS (The Cryogenic Dark Matter Search) collaboration [106] as detector material. However, the size of such ionization detectors are limited.

Scintillation

Scintillation detectors, e.g., sodium iodine (NaI) or liquid xenon (LXe), are the solution to accumulate large mass of detector material ($\approx 100kg$). However, it is more difficult to achieve radiopurity comparable to Ge detectors [103].

Moreover, scintillation detectors do not measure the elevation of the temperature in the crystal, but the light emitted by the electrons produced due to the ionization, thus the energy threshold for these detectors may be substantially higher than the thermal calorimeters [57].

Combinations of two different signals

Actually, most of the direct WIMP detection experiments use detectors with mixed techniques and measure simultaneously two signals. For example, for cryogenic detectors, the CDMS collaboration [106], investigate the heat-ionization signals and the CRESST (Cryogenic Rare Event Search using Superconducting Phase Transition Thermometers) collaboration [104] explores the heat-scintillation channel.

Combining information measuring from two different channels can offer a powerful event-by-event rejection method for the background discrimination down to 5 to 10 keV recoil energy [55]. Due to the quenching effect of the detector material, the ratio of the ionization or the scintillation signal to the heat signal is significantly different for the nuclear recoils and for the electron recoils. Similarly, nuclear recoils due to WIMP or neutron interactions have a much higher characteristic light over charge ratio than electron recoils due to electron and $\gamma - ray$ interactions [107]. Thus simultaneous measurements of two of the heat, the ionization, or the scintillation signals can be used to distinguish nuclear recoils induced by WIMPs from electron recoils induced by electron or $\gamma - ray$ interactions.

4.2.4 Background discrimination

As mentioned in the beginning of this chapter, due to the very low cross section of WIMPs on ordinary material, the event number of the elastic WIMP-nucleus scattering is very rare and the backgrounds coming from different sources are much larger. For example, cosmic rays and cosmic-ray induced γ-rays with energies in the keV to MeV range, radioactive isotopes in and around the detector (in the equipment) should be considered. Moreover, neutrons induced by cosmic muons can produce nuclear recoil events similar to the real events induced by WIMPs. Electron recoils from photons (x-ray and $\gamma - ray$ radiations) and electrons are also a major background. There are various ways to avoid these background signals (Noises) or to rectify the signals with background contributions. Some of them are described below:

Cosmic muons and underground laboratories

At ground level, approximately 10^3 cosmic muons pass through per square centimeter of the Earth's surface per day [103]. They can induce nuclear transmutations to unstable isotopes throughout the detector volume [103].

In order to protect from the penetrating cosmic muon flux, it is necessary to place the detector in deep underground. In underground laboratories such as the Soudan Underground Laboratory (the CDMS collaboration) in Minnesota in the USA, the Gran Sasso National Laboratory (the CRESST and DAMA collaborations) in Italy, the muon flux can be reduced by a factor of $10^5 - 10^7$ [103].

External natural radioactivity and (passive) shielding

External sources of radioactivity mean the radioactive isotopes in the rock around the underground laboratory and in the walls of the laboratory.

A shielding from external natural radioactivity can be achieved by surrounding the detector with thick absorbing material [103]: high-Z (Z is atomic number) materials like lead are very effective for stopping γ-rays with MeV energy, while low-Z materials are sufficient for stopping low energy γ-rays as well as α and β-radiations.

Internal natural radioactivity and radiopure materials

Beyond a thickness of 15 to 25 cm of lead shielding [103], one has to consider the internal radioactivity of the equipment, of the contamination near the detector or in the target material, and even of the lead shielding itself.

Internal radioactivity can be reduced very well by using detectors (and the other experimental equipment) made of radiopure materials. Archeological lead has also often been used since it has already been shielded from cosmic rays for about 2000 years.

Active background rejection

Except passive shielding around the detector, most experiments use also some different techniques for active background rejection.

Generally there are two different types of background discrimination. Statistical

rejections are used to ascertain which fraction of the total event sample comes from a well-defined type of background, but cannot tell for one individual event [103]. Moreover, this kind of rejections depends strongly on the theoretical predictions about the true signals induced by WIMP's and the background events.

On the other hand, the event-by-event rejections check each recorded event in the detector independently of the others and can be used to reject background events with an almost 100% certainty. However, in practice there is always a small probability that some background event may fake the signals induced by WIMP's.

Neutron induced nuclear recoils

Cosmic muons can induce neutrons in the inner lead shielding and such fast neutrons can induce nuclear recoils similar to those induced by WIMPs. So we have to shield the detector from these neutrons. Generally fast neutron shielding consists of moderators made of material with a high density of hydrogen, such as polyethylene or water [103].

Multiple-scatter events and array of detectors

The interaction between WIMPs and ordinary material is too weak, or, equivalently, the mean free path of a WIMP in ordinary matter is too long (of the order of a light-year [103]), so that WIMPs could never interact more than once in a single detector or two adjacent detectors. In contrast, the mean free path of a neutron or a high energy photon is of the order of one centimeter, thus multiple-scatter events produced by neutrons are more common [103].

Hence, an array of closely packed detectors (e.g., the tower with six detectors used by the CDMS experiment [106]) can efficiently identify these multiple-scatter events [103].

Electron recoils

Theoretically WIMPs interact only with the nuclei (through the coupling to quarks) and produce nuclear recoils, while, due to the electromagnetic interaction, the dominant radioactive backgrounds interact usually with the electrons and produce electron recoils. Therefore, the experiments which can discriminate between the events due to nuclear

recoils and events due to electron recoils can reject most radioactive background [108].

There are three ways to distinguish nuclear recoils from electron recoils. First, due to the quenching effect of the detector material, the ratio of the ionization or the scintillation signal to the heat signal is significantly different for nuclear recoils and for electron recoils. Thus one can measure simultaneously the heat signal and the ionization or the scintillation signal to distinguish the nuclear recoil events from the electron recoil events.

Second, the decay times of pulses for nuclear recoils may be different than that for electron recoils [108]. Thus some experiments use only a scintillation detector, but measure also the timing of the signals [108]. However, due to the limited resolution and discrimination power of this pulse shape analysis at low energies, this effect allows only a statistical background rejection [55]. This technique has been used by the DAMA (Dark Matter collaboration, in Italy) collaboration [109].

Third, the range of a electron recoil is of the order of μm and that of a nuclear recoil is only of the order of nm. Thus the nuclear recoils have a much larger energy loss per unit length dQ/dx, or equivalently, produce a much higher energy density, than the electron recoils. Therefore, some experiments are actually immune to electron recoils because the energy they deposit is not dense enough to trigger [108].

Surface events and self shielding

Due to their very long mean free path, WIMPs will interact uniformly throughout the detector volume. In contrast, due to the short mean free path of the high-energy photons and neutrons, for a detector with a large volume, the interactions induced by radiations originating from the surrounding material and surface contamination will occur mostly at the detector surface [103].

This self-shielding effect leads to the incentive of building large position-sensitive detectors in order to reject the surface events. Moreover, low-energy photons, α and β-rays have very short mean free path ($\leq$ mm), and can be rejected even if the position sensitivity is limited [103].

4.2.5 Cyrogenic detectors

As discussed above, a WIMP detector is constrained by three important requirements: low threshold, (ultra) low background, and high detector material mass [56]. In the following we will present briefly some important collaborations worldwide and summarize their recent results and plans in the near future.

CDMS

The Cryogenic Dark Matter Search (CDMS) collaboration [106] uses the Berkeley Center for Particle Astrophysics (CfPA) germanium cryogenic detector [57]. Their first test run was at the Stanford University Underground Facility [57], and now moved to the deep Soudan Underground Laboratory (Soudan mine) in Minnesota in the USA [110]. The Soudan mine has 780 m rock overburden [110], the surface muon flux is then reduced by a factor of 5×10^4 [110], and the neutron background is also reduced by a factor of $400(\sim 4 \times 10^{-4}/kg/day)$ [56].

It was the first experiment to operate a detector measuring simultaneously ionization and heat signals with a germanium/silicon crystal as the target material [56]. They developed Z(depth)-sensitive Ionization and Phonon (ZIP) detectors. The principle of their ZIP detector is basically the same as that of Ionisation detector, except that the heat sensor is replaced by a thin film sensor and thus able to detect phonons before their complete thermalization [103].

Their tower's with mixed Ge and Si detectors are powerful for subtracting the neutron background [110]. Except the neutron multiple-scatter events, while Ge and Si have similar scattering rates per nucleon for neutrons, the WIMP-nucleon scattering rate is expected to be $5 - 7$ times greater in Ge than in Si for all but the lowest-mass WIMPs. Moreover, the kinematics of neutron elastic scattering gives a recoil energy spectrum scaled in energy by a factor of ~ 2 in Si compared to Ge, whereas the factor would be ~ 1 or less for WIMP elastic scattering. All of these three methods can be used (together), in conjunction with Monte Carlo simulations, to statistically subtract any neutron background.

In the first Soudan run of the CDMS-II experiment (from October 11, 2003 to January $11, 2004$)[110], one tower with 4 Ge (each 250 g) and 2 Si (each 100 g) ZIP detectors has been operated for 52.6 live days, the recoil energy thresholds of these six detectors

were between 10 and 20 keV, only one candidate event with a recoil energy of 64 keV in one Ge detector has been measured. For a WIMP mass of $60GeV/c^2$, a $4 \times 10^{-7}pb$ upper limit on the spin-independent WIMP-nucleon cross section from Ge has been achieved. Meanwhile, thanks to the ^{73}Ge ($spin - \frac{9}{2}$) and ^{29}Si ($spin - \frac{1}{2}$) content of natural germanium and silicon, a $0.2pb$ upper limit on the spin-dependent WIMP-neutron cross section for a WIMP mass of $50GeV/c^2$ has also been achieved. These were the world's lowest limits on the WIMP-nucleon cross-section in the case of spin-independent interactions and spin-dependent interactions with neutrons.

In the second Soudan run (from March 25 to August 8, 2004) [111], two towers (one tower with 4 Ge and 2 Si detectors and the other one with 2 Ge and 4 Si detectors) have been operated for 74.5 live days and the recoil energy thresholds have been improved to be only 7 keV, one more candidate event with a recoil energy of 10.5 keV in one Ge detector has been measured. For a WIMP mass of $60GeV/c^2$, the upper limit on the spin-independent WIMP-nucleon cross section has been given as $1.6 \times 10^{-7}pb$ from Ge and $3.4 \times 10^{-6}pb$ from Si (see Fig. 4.1).

CRESST

The Cryogenic Rare Event Search using Superconducting Phase Transition Thermometers (CRESST) collaboration [104] uses heat-scintillation detectors with $CaWO_4$ crystal in the Gran Sasso National Laboratory in Italy. Their detector provides a good rejection of surface events as of photons due to the much larger light yield from all electron recoils relative to nuclear recoils [108].

The detector used in this collaboration uses the superconducting-normal phase transition due to the difference of the temperature. A thin superconducting film of tungsten (W) has been grown on a silicon detector and held just below the critical temperature. Heat produced by WIMP-nucleus scattering will change the film to its normal state and the change in resistance could be measured [57]. However,the threshold energy of such a scintillation detector is relatively higher than for an ionization detector. Thus a disadvantage of the CRESST heat-scintillation detector is that an event measured by the phonon channel but producing no light may mimic a WIMP signal [108].

In 2003 CRESST ran two prototype detectors for a couple of months without neutron shielding. A significant neutron background on the oxygen in their $CaWO_4$ detectors was observed [108] and the light yield for W recoils is significantly less than for Ca or

O recoils. This result indicates that WIMPs are expected to interact primarily with W nuclei, while neutrons will interact relatively more often with O and Ca nuclei [103].

In early 2004 they operated two 300 g CRESST-II prototype detector modules, 16 events have been recorded and a rate for nuclear recoil energy between 12 and 40 keV of (0.87 ± 0.22) events/kg/day has been obtained [112]. However, this is compatible with the rate expected from neutron background, and most of these events lie in the region of the phonon-light plane anticipated for neutron-induced recoils [112]. Moreover, a particularly strong limit for WIMPs with coherent scattering results from selecting a region of the phonon-light plane corresponding to tungsten recoils, where the best module shows zero events [112]. The sensitivity achieved by the CRESST-II experiment is given in Fig 4.2 .

DAMA

The Dark Matter (DAMA) collaboration [109] uses a scintillation detector with ~ 100kg NaI in the Gran Sasso National Laboratory in Italy [113]. With 1400 m rock overburden, the total muon flux is reduced to $\sim 1/m^2/hr$ (one order of magnitude lower than that of CDMS), the external γ-ray flux is reduced by a factor of 10^5.

They are the only collaboration which claimed to detect the signal of halo Dark Matter due to the annual modulation effect.They also published a WIMP mass $m_\chi \simeq 52GeV/c^2$ and a WIMP-proton cross section $\sigma_{\chi p} \simeq 7.2 \times 10^{-6} pb$ [113] under the standard assumptions of WIMP Halo (see Fig. 4.1).

They are running now the DAMA/LIBRA (Large sodium Iodide Bulk for Rare processes) experiment with totally $\sim$ 250 kg NaI [114].

Heidelberg-Moscow (HDMS)

The Heidelberg-Moscow collaboration [105] uses a $\sim$ 2 kg ^{76}Ge semiconductor ionization detector in the Gran Sasso National Laboratory in Italy and achieved a very low background count rate (≤ 0.2 event/kg/day) in the interval $10 - 40$keV, and a threshold energy $Q_{th} \simeq 4 - 10 keV_{ee}$ (equivalent to $\simeq 15 - 30$ keV recoil energy) [56].

They produced the first limits on WIMP searches and until recently had the best performance. However, without positive identification of nuclear recoil events, these experiments could only set limits, e.g., excluding sneutrinos as major component of the galactic halo [55].

4.2.6 Liquid noble gas detectors

Liquid noble gas detectors have the advantage of easier scaling to large masses since it is based on liquids [108]. They can also be allowed to operate in higher temperatures: 165 K for xenon, 87 K for argon, and 27 K for neon [115].

Due to its high-A value, liquid xenon (LXe) has been used by the ZEPLIN (The Zoned Proportional Scintillation in Liquid Noble Gases) collaboration [117] as the first liquid noble gas detector material. Recoils in the liquid noble gas such as Xe can induce both ionization and excitation of Xe atoms. An excitation produced by a nuclear recoil usually induces emission with a single photon, whereas that reduced by an electron recoil emits photons in form of a slow triplet, thus nuclear recoils have a faster pulse shape than electron recoils [108].

Besides xenon, argon and neon are also suitable detector materials. The effect of faster pulse shape is particularly clear in Ar and Ne, leading to their extremely good discrimination based on timing [107]. Moreover, the scintillation (light) over ionization (charge) ratio can be used additionally to discriminate the nuclear recoils from the electron recoils due to electron and γ-ray interactions.

However, discrimination of the radioactive contamination in the detector material, such as ^{85}Kr in liquid Xe (25 ppm Kr in natural Xe) or especially ^{39}Ar in liquid Ar [108] as well as of the surface radioactivity from the liquid container [103], and relatively larger threshold energies could be primary challenges for detectors using liquid noble gases.

ArDM

The Argon Dark Matter (ArDM) experiment at CERN [118] uses a ton-scale detector with liquid argon (LAr), which measures simultaneously the scintillation and the ionization signals [107].

With a recoil energy threshold of 30 keV and a sensitivity of $10^{-6}pb$ WIMP-nucleon cross section, the ArDM experiment has been expected to yield approximately 100 events per day per ton [107]. By improving the background rejection power and further limiting the background sources, a sensitivity of $10^{-8}pb$ (1 event per day per ton) would become reachable [107].

WARP

Similar to the ArDM experiment, the WIMP Argon Programme (WARP) experiment [119] also uses a dual-phase (gas-liquid) argon detector [108] in the Gran Sasso Underground Laboratory in Italy [115]. By using a strong electric field, ionization electrons are drifted out of the liquid argon into gaseous phase, where they are detected via the secondary luminescence [103]. The discrimination technique is based on both the pulse shape of the photon emissions and on the ratio of the scintillation to ionization energies [108].

Their first run of a 2.6kg ($1.87l$) prototype with a 96.5kg-day exposure resulted in no candidate events above the threshold energy 55keV [115] (see Fig. 4.1). Now the detector has been upgraded to total of 140kg ($\geq 100l$.) [115].

XENON

The XENON collaboration [120] uses also a dual-phase xenon time projection chamber (XeTPC) with 3D position sensitivity in the Gran Sasso Underground Laboratory in Italy. The XENON-10 experiment uses 15 kg liquid xenon, the background rate from ^{85}Kr contamination is reduced by a factor of 5000 by using a commercially available low-Kr (5 ppb) xenon, the self-shielding effect of LXe(Liquid Xenon) can reduce the background events in the central region of the LXe target by more than one order of magnitude for recoil energy below $50keV_{ee}$, (5 to 15 keV_{ee} corresponds to roughly 15 to 40 keV recoil energy) [121].

By measuring simultaneously the scintillation and the ionization produced by radiation in pure liquid xenon, the detector can discriminate signals from background down to $4.5keV_{ee}$ [122]. Between October $6, 2006$ and February $14, 2007$ the XENON experiment has been run for 58.6 live days and 10 events have been observed in the energy range 4.5 to $26.9keV_{ee}$. However, none of these events are likely to be WIMP interactions [122].

Their newest result gives a 90% C. L. upper limit on the spin-independent WIMP-nucleon cross section of $8.8 \times 10^{-8}pb$ for a WIMP mass of $100GeV/c^2$ [122], a factor of 2.3 lower than the limit achieved by CDMS-II experiment. For a WIMP mass of $30GeV/c^2$, the limit is $4.5 \times 10^{-8}pb$ [122] (See Fig 4.1).

ZEPLIN

The Zoned Proportional Scintillation in Liquid Noble Gases (ZEPLIN) collaboration [117] first used a liquid xenon scintillation detector in the Boulby Laboratory ($1070\ m$ underground) in the United Kingdom.

ZEPLIN-I was a single-phase experiment with 6 kg Xe, so it could not collect the ionization signals, but depended solely on the pulse shape discrimination [108]. In an exposure of 293 kg-day, no excess consistent with nuclear recoils was seen [108]. However, the published limits are somewhat controversial, because their calibration results of the neutron recoil discrimination do not appear to be convincing enough to consider the limits set on the WIMP signal to be as reliable as the ones set by the cryogenic experiments [55]. Actually, with only 1.5 photo-electron per keV and a three- fold coincidence, searching for the WIMP signal in the $2 - 10keV_{ee}$ region is for ZEPLIN-I quite challenging [55].

ZEPLIN-II has been upgraded to a dual-phase experiment with 31 kg Xe [124]. In the first run with 225 kg-day exposure, 29 events have been observed in an acceptance window defined between $5keV_{ee}$ and $20keV_{ee}$. With a summed expectation of 28.6 ± 4.3 γ-ray and radon progeny induced background events, these figures provide a 90% C. L. upper limit to the number of nuclear recoils of 10.4 events in this acceptance window, which converts to a spin-independent WIMP-nucleon cross-section of $6.6 \times 10^{-7}pb$ for a WIMP mass of $65GeV/c^2$ (see Fig.4.1). For the second run a sensitivity of $2 \times 10^{-7}pb$ has been achieved (see Fig. 4.2).

4.3 Indirect Detection

In the previous section we discussed the methods of direct detection of WIMP Dark matter. Here we will throw light on the indirect methods of WIMP Dark matter detection. In supersymmetry, neutralinos are classified as Majorana particles (they are their own antiparticle) and therefore annihilate with each other, giving off various products which can be detected. Hence a potential signal for the existence of dark matter is WIMP-WIMP annihilation. This technique is called indirect detection, since we are not actually detecting the WIMPs themselves. Because the annihilation rate of WIMPs is proportional to the square of the dark matter density ($\Gamma_A \propto \rho_{DM}^2$), natural places to look for dark matter annihilations are those expected to have high WIMP densities, such as the Sun, Earth, and galactic center. Annihilation products include gamma-rays, neutrinos, and antimatter [1].

4.3.1 Gamma-Rays

Gamma-rays from WIMP annihilation are believed to occur most frequently in the galactic center. One way this process can take place is through a WIMP annihilation yielding a quark and antiquark, which then produce a particle jet from which a spectrum of gamma rays is released. The quark antiquark fragmentation process has been thoroughly studied at accelerators and is well understood; the creation and propagation of gamma rays from such a jet is a fairly predictable process (compared to, for example, the random walk of charged antimatter particles through space). A second form of gamma-ray production is the decay of WIMPs directly to gamma-rays, ($\chi\chi \rightarrow \gamma\gamma$),which produces gamma-rays (a gamma ray line) that are proportional to the mass of the WIMPs involved. Since typical WIMP masses can be of the order of 100s of GeV, these are extremely high energy gamma rays. Although the flux is small and quite difficult to detect, observing such a gamma-ray line would be an obvious indication for dark matter annihilation and the WIMP mass [1].

As a gamma-ray enters an indirect detection device, it first passes through an anti-coincidence shield which limits the amount of charged particles entering the detector. The gamma-ray then encounters conversion foils, which are thin sheets of heavy nuclei that convert the photon to a e^+e^- pair. A calorimeter tracks the energies of the positron and electron, while particle tracking detectors measure their trajectories. The signature of a gamma-ray event is then a registered energy with nothing triggering the anti-coincidence shield, and the indication of two particles (the positron and electron) coming from the same location.

The EGRET Collaboration reported an excess of gamma rays in 1998, pointing toward already accepted characteristics of dark matter: a $50 - 70$ GeV WIMP mass and a ring of concentrated dark matter at a radius of 14 kpc from the galactic center (which would nicely answer for our flat rotation curves) [125]. This discovery is initially encouraging, but as Bergstrom et al. have shown, observed antiproton fluxes would have to be much larger if these excess gamma rays are being produced by neutralino or generic WIMP self annihilation [126]. For this reason and others, EGRET's results remain controversial.

4.3.2 Neutrinos

Neutrinos can be another important product of WIMP annihilation. As WIMPs travel through the universe and through matter, they lose small amounts of energy due to scattering off nuclei. Therefore,WIMPs can gather at the centers of large gravitating bodies, increasing their density until their annihilation rate equals half the capture rate (two WIMPs are needed for annihilation, where only one is needed for capture). For many of the primary particle physics models, the WIMP annihilation and capture rates are at (or nearly at) equilibrium in the Sun, a conveniently close object to observe. This equilibrium should allow for a steady annihilation rate, and therefore a constant flow of neutrinos emanating from within the Sun (we study only the neutrinos and not other products of annihilation because neutrinos interact so weakly that most escape from the Sun or body in question). Why not, then, study neutrinos coming from WIMP annihilations within the Earth, an even closer gravitating body? The earth (in most models) has not reached such an equilibrium and thus does not provide a flux of neutrinos; it is less massive than the Sun, so it causes less WIMP scattering and a much smaller gravitational potential well. Neutrino telescopes therefore usually focus on neutrino flux coming from the Sun, rather than the Earth.

The differential neutrino flux from WIMP annihilation is given by [1]

$$\frac{dN_\nu}{dE_\nu} = \frac{\Gamma_A}{4\pi D^2}\Sigma_f B_X^f \frac{dN_\nu^f}{dE_\nu} \tag{4.26}$$

where Γ_A is the annihilation rate of WIMPs in the Sun and D is the distance of the detector from the source (the central region of the Sun and Earth),f is the WIMP pair annihilation of final states, and B_X^f are the branching ratios of the final states. $\frac{dN_\nu^f}{dE_\nu}$ are the energy distributions of neutrinos generated by the final state f [127]. Depending on the WIMP's mass and composition, annihilation processes include $\chi\chi \rightarrow t\bar{t}, b\bar{b}, c\bar{c}, W^+W^-, and\ \tau^+\tau^-$, which then decay to neutrinos among other products. For neutralinos or generic WIMPs lighter than $W^\pm$, annihilation to $b\bar{b}$ and $\tau^+\tau^-$ are the most common processes, yielding neutrinos with energies around 30 GeV. WIMPs with higher masses annihilate to Higgs and gauge bosons, top and bottom quarks, and muons, leading to neutrinos of masses that are much easier to detect (about half of the WIMP mass). Detection, then, depends heavily on the WIMP mass, as well as the annihilation rate, density within the Sun, and other factors.

As neutrinos pass through the Earth, they sometimes interact with the hydrogen and oxygen and other atoms around the optical modules of a neutrino detector. Electrons, muons, and taus produced by such events are extremely energetic and are traveling faster than the speed of light in the medium; the particles are then detected optically due to the Cherenkov radiation they emit.

Because neutrinos are so weakly interacting, neutrino telescopes must be massive to detect a significant signal. AMANDA-II is a neutrino detector 1500 to 2000 meters underground within the ice of the South Pole where Cherenkov radiation can travel and be seen easily by optical modules. This experiment has not detected statistically significant results from the direction of the Sun, but has helped to place firm limits on the muon flux[128]. Super- Kamiokande (Super-K) is another indirect detection experiment, located underground in the Kamioka-Mozumi mine in Japan. The detector consists of $50,000$ tons of water and detects Cherenkov radiation from incoming muons as well. Super-K looks in the direction of the Sun, earth, and galactic center, and, like AMANDA, has not detected any excess of muon rates above the expected background [129].

4.3.3 Antimatter

Antimatter can be a excellent signal of WIMP annihilation precisely because antimatter is relatively rare cosmically, and many of the astrophysical processes which create antimatter are well understood. For example, the annihilation of WIMPs can also produce antiprotons via $\chi\chi \rightarrow q\bar{q}$ through hadronization (where the dominate annihilation process yields b quarks and antiquarks), and positrons through secondary products of the annihilation such as W^+W^- (and ZZ), where W (or Z)$\rightarrow e^+\nu_e$. Unlike gamma-rays and neutrinos, these products are charged and thus affected by magnetic fields within space and also lose energy due to inverse Compton and synchrotron processes, so we cannot make any conclusions about where the annihilations occurred. We therefore study the flux of antimatter particles from the galactic halo as a whole, rather than assume dense areas such as the galactic center or large bodies.

Experiments searching for antimatter must be located near the top of the Earth's atmosphere; various other cosmic rays and their consequential particle showers create too large and uncertain of a background to make conclusive analyses. It is important, however, to still consider and subtract any background caused by cosmic rays that reach the edges of our atmosphere. In 1994, the HEAT Collaboration detected an excess of cosmic ray

positrons of energies around 10 GeV possibly caused by neutralino self-annihilation, and confirmed this signal again in 2000 [130]. A boost factor, however, must be applied to the WIMP annihilation rate of a smooth halo in order to match the HEAT data; this is perhaps an indication that we exist within an extremely clumpy halo, or that there are other unknown sources of antimatter. The Balloon-borne Experiment with Superconducting Spectrometer (BESS) also detected antiprotons with energies up to 4GeV during its nine flights over several years [131].

The results from the PAMELA (a Payload for Antimatter Matter Exploration and Light-nuclei Astrophysics) satellite-borne experiment's flight from July 2006 February 2008 were released. The collaboration found that the positron fraction increases sharply over much of the range of $1.5 - 100$ GeV and thus concluded that a primary source, either an astrophysical object or dark matter annihilation, must be present to account for the abundance of cosmic-ray positrons [132].The data from PAMELA also require heavy WIMP candidates or large boost factors associated with nonuniform clumps in the dark matter distribution, thus constraining the nature of the possible dark matter. ATIC (Advanced Thin Ionization Calorimeter), a balloon-based experiment, also reported an excess of e^- or e^+ at $300 - 800$ GeV.However, recent results from Fermi [133] and HESS [134] (the High Energy Stereoscopic System, a set of four Cherenkov telescopes in Namibia) do not see the same electron-positron excess of ATIC leaving the issue far from settled (however, Fermi does see an excess similar to that seen by PAMELA). Further data is necessary to determine if excess gamma ray and antimatter fluxes are indeed signals of dark matter annihilation or signatures of local astrophysical objects and backgrounds.

4.4 Production of Dark matter in Accelerators

It is an established fact that if Dark matter particles were produced in the early universe then it is possible that, we may be able to produce them at particle accelerators. Producing and detecting dark matter particles in an accelerator would be a huge step toward confirming the existence of dark matter. If we assume that R-parity is conserved and that the dark matter is the neutralino and thus the LSP, then a signal in an accelerator will have several distinctive features. When SUSY particles are created, they will decay to the LSP and most likely escape the detector. As the LSP leaves the collision space, it will carry with it energy and momentum which can be detected as missing energy and momentum. Similar signatures of missing energy would be detected if the dark matter were Kaluza-Klein

excitations or other exotic particles.

The accelerators may also produce other particles related to the Dark matter particles, which can help us to understand the physics behind Dark matter. We are expecting the LHC (Large Hadron Collider) experiment may provide us the breakthrough in the near future.

4.5 Prospects of Detection

So far we did not obtain any convincing signal from experiments searching for Dark matter particles. In the future, detector technique, better sensitivities as well as better background discrimination, will be improved. We need also some new ideas for detector building as well as application of experimental data.

The CDMS collaboration has achieved a (so far the best) sensitivity of $\sim 10^{-7}$pb for spin-independent WIMP-nucleon cross section and of $\sim 10^{-1}$ pb for spin-dependent WIMP-neutron cross section. Together with the other collaborations described above, direct WIMP detection experiments have started to probe some possible regions in the parameter space predicted by some supersymmetric models. For next-generation detectors, sensitivities will be upgraded down to$\sim 10^{-10}$ pb.and, in long term, even $\sim 10^{-12}$ pb, and the corresponding WIMP-nucleus scattering event rate is then ~ 5 events/ton/yr for Ge [55], as needed to probe large regions of MSSM parameter space. The total mass of detector material will also be improved to the ton scale. For example, the ~ 100 kg Xe detector of the XENON and XMASS collaborations. The CDMS collaboration is also preparing for their Super CDMS projects with maximum 1100 kg target mass, while the CRESST and the EDELWEISS collaborations will also build to a larger collaboration EURECA (European Underground Rare Event search with Calorimeter Array).

A nearly perfect background discrimination capability for next-generation detectors is also necessary. The ultimate neutron background will only be identified by the multiple interactions in a finely segmented or multiple interaction sensitive detector, or by operating detectors containing different target materials within the same setup [55]. Furthermore, the measurement of the recoil directions of the target nuclei would provide additional information on the distribution of WIMPs in our Galaxy [108].

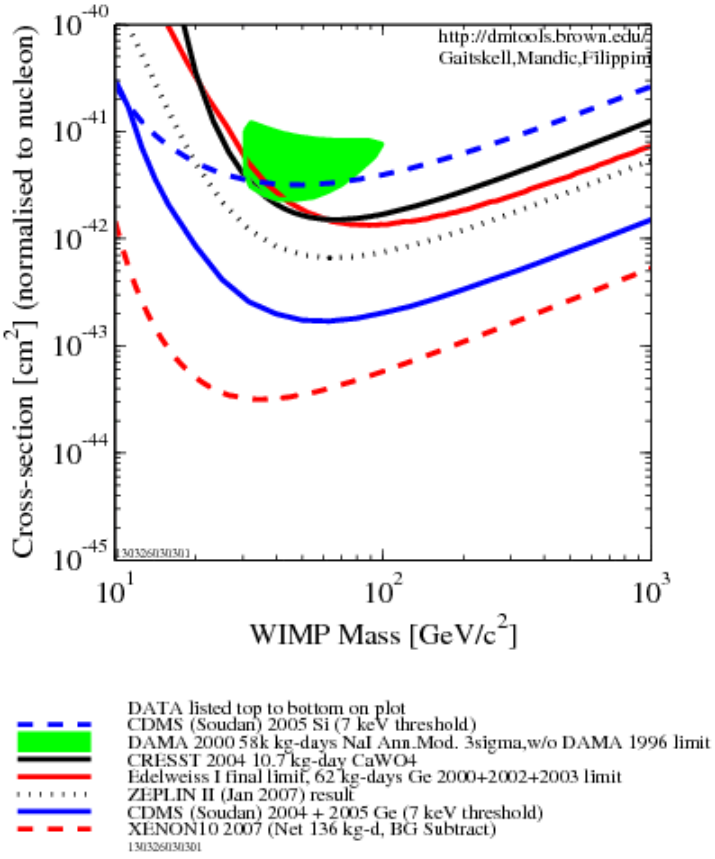

Figure 4.1: The curves show the sensitivities of (the exclusion limits on) the spin- independent WIMP-nucleon cross section versus WIMP mass achieved by various collaborations [123].

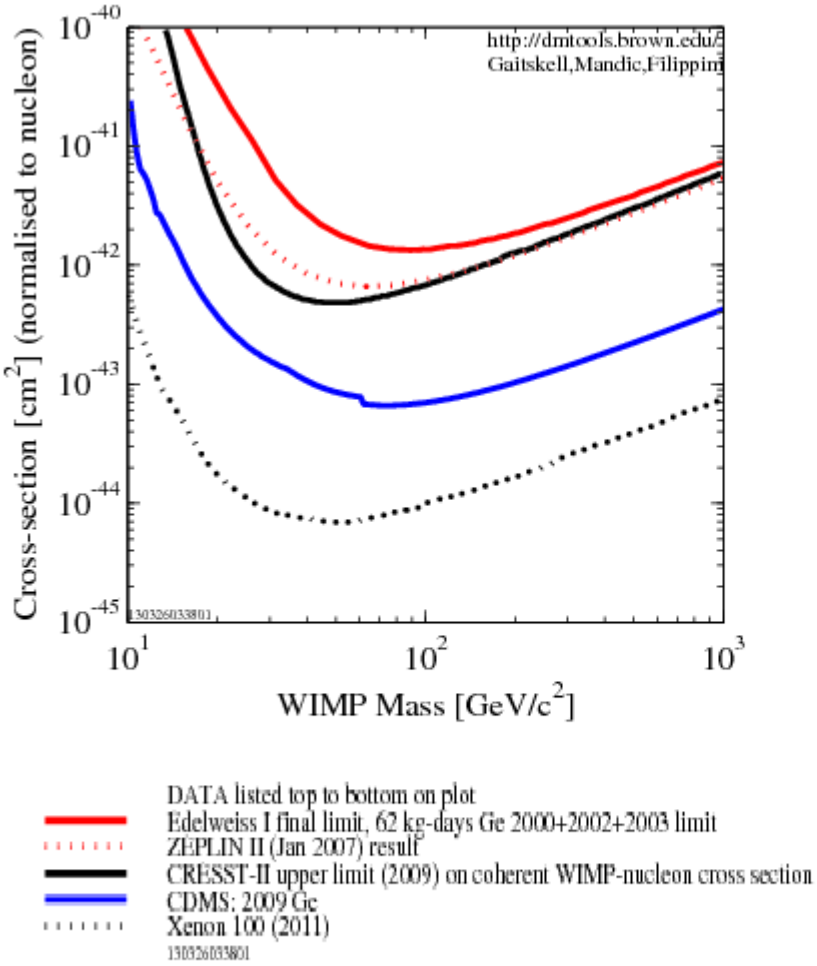

Figure 4.2: The curves show the sensitivities of the spin-independent WIMP-nucleon cross section versus WIMP mass recorded by various collaborations recently [123].

Chapter 5

Summary and Conclusions

Dark matter came about as a possible answer to observational problems, not as a theoretical prediction from some cosmological theory. While it is true that dark matter hasn't been observed in a laboratory as yet, the astrophysical and cosmological evidence for existance of dark matter is overwhelming. Perhaps the most striking are the multiple lines of evidence which point to the need for dark matter. Elemental abundances from Big Bang Nucleosynthesis and fundamental anisotropies in the Cosmic Microwave Background Radiation both predict very similar baryon (ordinary matter) abundances, yet each describes a completely separate era in the history of the Universe in which very different physical processes are occurring. Dark matter is necessary to describe both galaxies and clusters of galaxies, and is a necessary ingredient in the formation of large-scale structure. Current estimates suggest that of all the energy, matter density of our universe, Luminous matter accounts for only 4%, Dark matter accounts for about 23% and the rest 73% is carried by Dark energy (not the subject of this study).

The main aim of this work is to present a thorough review of the present status of Dark matter problem, motivation for studying Dark matter combined with an explaination of physics of Dark matter. For the sake of clarity, we divided the study into three parts: Begining with the description of the scientific discoveries and events which support the existence of Dark matter in our universe, we discussed Zwicky 's findings about the dynamics of coma cluster and the other contributions detailing the study of rotation curves of galaxies and clusters of galaxies leading to signatures of Dark matter.

Having argued that dark matter does exist in our universe though we have only indirect evidences, we analyze the composition of Dark matter in chapter 2. If only we

assume that Dark matter has the same composition as ordinary matter, the difference being that Dark matter does not radiate in any part of electromagnetic spectrum, then we can possibly state that Dark matter is baryonic in nature. The baryonic Dark matter candidates, commonly known as MACHOs (Massive Astrophysical Compact Halo Objects), include Black Holes, Neutron stars, White dwarfs and Brown dwarfs, All of these are either the star remainents or a failed star with no signs of thermonuclear burning inside their cores. So the compact objects do not radiate in any part of electromagnetic spectrum, hence it is very difficult to identify or locate these compact objects by using tools of visual astronomy. However, these objects interact with their surrounding matter by exerting enormous gravitational pull on it. To detect these objects scientists use various methods and techniques, prominant among which include: (1) study of rotation curves of galaxies. (2) Gravitational lensing and (3) Study of Accertion disks. The MACHO collaboration has discovered large number of these compact objects but their number is not too large to account for all the Dark matter in our universe. Thus it seems unlikely that Dark matter can be only baryonic in nature. Infact, only a small fraction of the baryonic matter can be dark matter.

The inability of astrophysical candidates to account for all the missing mass compels us to explore the other possible candidates from different branches of physics. Since particle physics helps us to understand the composition of material objects, a natural choice to search for the possible candidates of Dark matter is particle physics. These candidates are generically referred to as WIMPs (Weakly Interacting Massive Particles). The standard model of particle gives only neutrino as a vialable candidate. However, the neutrino, being relativistic, is inconsistent with the simulations of structure formation. This neutrino though may account for a very small fraction of dark matter but cannot account for all the Dark matter. The supersymmetry comes to our rescue, because it doubles the number of available particle candidates.

Among the Cold Dark matter (non relativistic) candidates, neutralinos, sneutrinos and axions are described in chapter 2. Though neutralinos and axions account for the considerable amount of Dark matter theoretically, but it is very difficult to detect these particles due to their weak interaction with the ordinary matter. We also discussed the other possible candidates like dark baryons. However, of all the dark matter candidates from particle physics, the neutralino appears to be the most promising one.

Having identified the various candidates of dark matter, we then discussed the distribution of Dark matter in the universe in chapter 3. We discussed the dynamics of various

galaxies and clusters of galaxies. It follows from the observational evidence that the distribution of Dark matter is far from uniform. A larger portion may reside in the galaxy halos and even larger part in cluster cores. Large but uncertain content of dark matter has been reported in the local group. There are possibilities that galaxies exist in which there are so few stars that the galaxy is almost completely dark matter. However, there exist a modest number of objects and systems (e.g. open and globular star clusters) where little or no dark matter is present.

Since the nature of dark matter is not known, its detection is a huge challenge. In chapter 4, we discussed various detection techniques being employed. We started with the description of direct dark matter detection in the laboratory. The WIMPs after striking our detector may get scattered by the nucleons of the detector and the nucleon recoil can help us to calculate the energy and mass of the WIMP particle. We discussed the techniques used by various collaborations for the direct detection of WIMPs. We also discussed the other techniques apart from direct method, being employed to detect the Dark matter. These include indirect method and production of Dark matter signals in the particle accelerators. The detection of Dark matter in the laboratory is still a distant dream because we have so far not been able to detect and confirm the existence of WIMPs. However, in the last decade lot of progress has been made and that day is not far away when we will be able to detect these WIMPs. At present we face lot of challenges regarding the sensitivity and efficiency of our instruments. The Large Hadron Collider experiment may give us the breakthrough in near future.

The microscopic properties of dark matter are as much a mystery now as they were in the 1930's when the existence of dark matter was first hypothesized. However, our current understanding makes it increasingly clear that dark matter is indeed a fundamental and necessary component of our universe. The main conclusions of this study are enlisted below:

- Dark matter does exist, the astrophysical and cosmological evidences of Dark matter are too strong to be ignored.

- Dark matter is necessary to describe the motions of stars in galaxies and clusters of galaxies, and is a necessary ingredient in the formation of large-scale structure. In fact, our understanding of universe is incomplete with out the understanding of dark matter. Dark matter accounts for about 23% of the energy matter density of our universe, which is nearly 6 times the luminous matter.

- Dark matter distribution is not uniform. It is more likely to reside in the cores of clusters and in the halos around the galaxies.

- The exact composition of Dark matter is still unknown. However the theory of supersymmetry (SUSY) provides a solid frame work for attempting to understand dark matter.

- Most of the Dark matter in the Universe is non-baryonic. The baryonic candidates of Dark matter are too small in number to account for a substantial amount of the Dark matter.

- Since dark matter cannot be seen or touched, all possible candidates ranging from subatomic particles with masses 10^5 times less than an electron to black holes with masses millions of times that of the sun have been proposed. However, very little success has so far been achieved in identifying the true candidates of Dark matter.

- Of all of the particle candidates for dark matter, the best motivated is the neutralino. It is a typical WIMP: electrically neutral, weakly interacting, and massive.

- Dark matter, of course, is not completely understood and faces challenges. The primary challenge is that it still remains undetected in the laboratory. We only have indirect evidences.

- The results of present day experiments like DAMA, ZEPLIN, CRESST and other collaborations are highly motivating indicating a breakthrough in near future. The discovery of WIMP's will revolutionise the whole physics.

5.1 Future Outlook

Nearly a decade back (in 2004) Nobel Prize winning physics professor, Carlo Rubbia, had claimed in a conference in UK that the detection of dark matter may be possible within a decade. Since that decade is about to end and we still have no direct observational evidence of dark matter, we shall use our words with caution. We can say for sure that the next decade of dark matter research is going to be exciting for both astronomers

and particle physicists. The reason we are optimistic about a breakthrough is the fact that the rate of sensitivity increase in direct detection experiment is steeper than allowed by Moore's law and experiments operating deep underground have reached sensitivities to probe the predicted parameter space of beyond-standard-model particle physics theories. Large Hadron Collider (LHC) may reveal signatures of physics beyond the standard model but determining the nature of dark matter using LHC data alone may be too big a challenge. It is important that a cross desciplinary approach is used to tackle the dark matter problem. Cosmology comes handy, particularly after the highly successful WMAP and PLANCK satellite missions which have revealed a lot about the existance of dark matter. Besides a number of direct and indirect detection techniques and experiments sensitive to different particle properties are required. A large number of direct dark matter detection techniques which include Solid-state cryogenic detectors, Noble liquid detectors, Scintillating crystals, Superheated liquid detectors are in operation and a lot has been learnt from such experiments. Many large-scale direct detection experiments including improvements in the already exisiting ones are planned for the next decade which promise to revolutionize our understanding of the dark matter.

Bibliography

[1] Katherine Garrett and Gintaras Duda, *Advances in Astronomy*. ID968283 (2011).

[2] Annika H.G. Peter, *arxiv:astro-ph/1201.3942v1*. (2012).

[3] Matts Roos, *arxiv:astro-ph/1001.0316v2*, (2010).

[4] J. H. Oort, *Bulletin of the Astronomical Institutes of the Netherlands*. **4**, 249 (1932).

[5] F. Zwicky, *Helvetica Physica Acta*. **6**, 110-127 (1933).

[6] V. C. Rubin, *Scientific American*. **248**, 96-108 (1983).

[7] See *http://www.hep.shef.ac.uk*.

[8] D. Walsh, R. F. Carswell, and R. J. Weymann, *Nature*. **279**, 381-384 (1979).

[9] R. Lynds and V. Petrosian, *The Astrophysical Journal*. **336**, 1-8 (1989).

[10] A. G. Bergmann, V. Petrosian, and R. Lynds, *Astrophysical Journal*. **350**, 23-35 (1990).

[11] L. Kawano, *NASA STI/Recon Technical Report*. **92**, 25163 (1992).

[12] R. H. Cyburt, *Physical Review D*. **70**, 2 (2004).

[13] A. A. Penzias and R. W. Wilson, *The Astrophysical Journal*. **142**, 419-421 (1965).

[14] G. F. Smoot, C. L. Bennett, A. Kogut et al., *Astrophysical Journal*. **396**, 1-5 (1992).

[15] N. Jarosik et al., "Seven-year Wilkinson Microwave Anisotropy Probe (WMAP1) observations: sky maps, systematic errors, and basic results", *http://arxiv.org*/abs/1001.4744.

[16] K. N. Abazajian, J. K. Adelman-Mccarthy, M. A. Agueros et al., *Astrophysical Journal*. **182**, 543-558 (2009).

[17] D. J. Eisenstein, I. Zehavi, D.W. Hogg et al., *Astrophysical Journal*. **633**, 560-574 (2005).

[18] S. Cole, W. J. Percival, J. A. Peacock et al., *Monthly Notices of the Royal Astronomical Society*. **362**, 505-534 (2005).

[19] W. J. Percival, B. A. Reid, D. J. Eisenstein et al., *Monthly Notices of the Royal Astronomical Society*. **401**, 2148-2168 (2010).

[20] C. evoli et al., *arxiv:astro-ph/1210.6845v1*, (2012).

[21] M. Boylan-Kolchin, V. Springel, S. D. M. White et al., and G. Lemson, *Monthly Notices of the Royal Astronomical Society*. **398**, 1150-1164 (2009).

[22] T. Di Matteo, J. Colberg, V. Springel, L. Hernquist et al., *Astrophysical Journal*. **676**, 33-53 (2008).

[23] P. J. E. Peebles, *The Astrophysical Journal*. **263**, L1-L5 (1982).

[24] A. Jenkins, C. S. Frenk, F. R. Pearce et al., *Astrophysical Journal*. **499**, 20-40 (1998).

[25] Paczynski, *Ann. Rev. Astron. Astrophys*.**34**, 419 (1996).

[26] MOA Collaboration, *http://www.phys.canterbury.ac.nz/moa/*.

[27] A. Becker et al., *IAU Symposium*. **225**, 357-362 (2005).

[28] C. Alcock, R. A. Allsman, D. R. Alves et al., *Astrophysical Journal*. **542**, 281-307 (2000).

[29] P. Tisserand, L. Le Guillou, C. Afonso et al., *Astronomy and Astrophysics*.**469**, 387-404 (2007).

[30] D. Clowe, M. Bradac, A. H. Gonzalez et al., *Astrophysical Journal*. **648**, 109-113 (2006).

[31] M. Bradac, S. W. Allen, T. Treu et al., *Astrophysical Journal*.**687**, 959-967 (2008).

[32] *http://www.nasa.gov/mission-pages/hubble/science/dark-matter-core.html*.

[33] S Penny et al., *MNRAS*.**393**, 1054 (2009).

[34] M. J. Jee, H. C. Ford, G. D. Illingworth et al., *Astrophysical Journal*.**661**, 728-749 (2006).

[35] C. J. Hailey et al., *Adv. Sp. Res.*. doi:10.1016/j.asr.2011.04.025 (2011).

[36] T. Banks et al., *ArXiv:1007.5515*. (2010).

[37] E. Komatsu et al., *Ap.J*. **180**,330 (2009).

[38] A.G. Riess et al., *Ap.J*. **659**, 98 (2007).

[39] M. Kowalski et al., *Ap.J*. **686**, 719 (2008).

[40] M. Herreo, *ArXiv:hep-ph/9812242*, (1998).

[41] Zeilik, Michael, and John Gaustad, *Astronomy: The Cosmic Perspective*. New York: John Wiley & Sons (1990).

[42] Stuart L. Shapiro and Saul A. Teukolsky, *The Physics Of Compact Objects*. John Wiley and Sons.

[43] J. R. Bond, G. Efstathiou and J. Silk, *Physical Review Letters*. **45**, 1980-1984 (1980).

[44] M. Iye, K. Ota, N. Kashikawa et al., *Nature*.**443**, 186-188 (2006).

[45] D. N. Spergel et al., *ApJ*. **148**, 175, (2003)

[46] G. Bertone, *Nature*. **468**, 389 (2010)

[47] C. Amsler, M. Doser, M. Antonelli et al., *Physics Letters B*. **667**, 1-6 (2008).

[48] J. Wess and J. Bagger, *Supersymmetry and Supergravity*. Princeton University Press (1992).

[49] U. Amaldi, W. De Boer, and H. Furstenau, *Physics Letters B*.**260**, 447-455 (1991).

[50] P. Langacker and M. Luo, *Physical Review D*. **44**, 817-822 (1991).

[51] T. Falk, K. A. Olive and M. Srednicki, *Physics Letters B*. **339**, 248-251 (1994).

[52] L. J. Hall, T. Moroi and H. Murayama, *Physics Letters B*. **424**, 305-312 (1998).

[53] E. J. Chun, H. B. Kim and J. E. Kim, *Physical Review Letters*. **72**,1956-1959 (1994).

[54] S. Borgani, A. Masiero and M. Yamaguchi, *Physics Letters B*. **386**, 189-197 (1996).

[55] M. Drees and G. Gerbier, Review of Particle Physics, *J. Phys. G: Nucl. Part. Phys*. **33**, 22, Dark Matter (2006).

[56] M. de Jesus, *Int. J. Mod. Phys*.**A 19**, 1142 (2004).

[57] G. Jungman, M. Kamionkowski and K. Griest, *Phys. Rep*. **267**, 195 (1996).

[58] R. D. Peccei and H. R. Quinn, *Phys. Rev. Lett.* **38**, 1440 (1997)

[59] M. S. Turner, *arXiv:astro-ph/9904051* (1999).

[60] V. Trimble, *Annu. Rev. Astron. Astrophys*. **25**, 425 (1987).

[61] K.C. Freeman, *Ap. J*. **160**, 811 (1970).

[62] M. Persic, P. Salucci and F. Stel, *MNRAS*. **281**, 27-47 (1996).

[63] P. Salucci, M. Persic, *ASP Conf. Ser, Astron.Soc.Pac.San Francisco*.**1**, 117 (1997).

[64] I. Yegorova and P. Salucci, *MNRAS*. **377**, 507 (2007).

[65] F. J. Navarro, S. C. Frenk and D. S. White, *Ap. J*.**462**, 563 (1996).

[66] A. Burkert, *Ap. J*. **447**, L25 (1995).

[67] Moore et al., *MNRAS*. **310**, 1147 (1999).

[68] Fukushinge and Makino, *Ap. J*. **557**, 533 (2001).

[69] Hayashi et al., *MNRAS*.**355**, 794 (2004).

[70] De Vaucouleurs, *Ann. d' Astrophys*. **11**, 247 (1948).

[71] Carollo et al., *Ap. J.***441**, L25 (1995).

[72] F. De Poalis, G. Ingrosso and F. Strafela, *Ap. J*. **438**, 83 (1995).

[73] G. Bertin, R. P Saglia and M. Stiavelli, *Ap. J*. **384**, 427 (1992).

[74] F. Schweizer, J. H. Van Gorkom and P. Seitzer, *Ap. J*. **338**, 770 (1989).

[75] Bertola et al., *Ap. J*. **416**, 248 (1993).

[76] J. C. Forman, C. Jones and W. Tucker, *Ap. J*. **293**, 102 (1985)

[77] O' Sullivan and T. J. Ponmam, *MNRAS*. **354**, 935 (2004).

[78] T. G. Briemer and R. H. Sanders, *Astron. Astrophys*. **294**, 96 (1995).

[79] C. Kochanek, *Ap. J*. **445**, 559 (1995).

[80] Mould et al., *Astron. J*. **99**, 1823 (1990).

[81] M. Mateo et al., *IAU*. **149**, (1992).

[82] Piatek and Pryor, *Ap.J*. **66**, 8-10 (1995).

[83] Salucci and Persic, *Astron. Astrophysics*. **186**, 432 (1997).

[84] Dalcanton et al., *Ap. J*. **482**, 659 (1997).

[85] W.H. Herschel, *In Collected Works*. **1**, 157 (1784).

[86] J. Felten, *Comments Astrophysics*.**11**, 53 (1986).

[87] E. Giraud, *Astron. Astrophys*. **167**, 42 (1986).

[88] G.D. Forets et al., *Ap.J*. **280**, 15 (1984).

[89] S.M. Kent and W.L. Sargent, *Astron.J*. **88**, 697 (1983).

[90] G. Bothen et al., *Ap.J*. **268**, 47 (1983).

[91] D.P. Schneider et al., *Astron.J*. **92**, 523 (1986).

[92] J. Heisler et al., *Ap.J*. **298**, 8 (1985).

[93] S.J. Millington and J.V. Peach, *MNRAS*. **221**, 15 (1986).

[94] D. Merritt, *Ap.J*. **313**, 121 (1987).

[95] D. Fabricant et al., *Ap.J*. **308**, 530 (1986).

[96] R. Giovanelli et al., *Ap.J*. **300**, 77 (1986).

[97] H. Rood, *Rep. Progr. Phys*. **44**, 1078 (1980).

[98] S. Nincovich, *Astrofizika*. **20**, 150 (1984).

[99] W. Forman et al., *Ap.J. Lett.*. **293**, 102 (1985).

[100] M. W. Goodman and E. Witten, *Phys. Rev. D*. **31**, 3059 (1985).

[101] Y.Ramachers, *Nucl. Phys. Proc. Suppl*. **118**, 341 (2003).

[102] EDELWEISS Collab., V. Sanglard et al., *Phys. Rev. D*. **71**, 122002 (2005).

[103] J. Gascon, *arXiv:astro-ph/0504241* (2005).

[104] See *http://www.cresst.de/*.

[105] See *http://www.mpi-hd.mpg.de/non acc/dm.html*.

[106] P. Gondolo and G. Gelmini, *Phys. Rev. D*. **71**, 123520 (2005).

[107] L. Kaufmann and A. Rubbia, *J. Phys. Conf. Ser*. **60**, 264 (2007).

[108] R. W. Schnee, *AIP Conf. Proc*. **903**, 8 (2007).

[109] See *http://people.roma2.infn.it/dama/web/home.html*.

[110] CDMS Collab., D. S. Akerib et al., *Phys. Rev. D*. **72**, 052009 (2005).

[111] CDMS Collab., D. S. Akerib et al., *Phys. Rev. Lett*. **96**, 011302 (2006).

[112] CRESST Collab., G. Angloher et al., *Astropart. Phys*. **23**, 325 (2005).

[113] DAMA Collab., R. Bernabei et al., *Phys. Lett.B*. **480**, 23 (2000).

[114] DAMA Collab., R. Bernabei et al.,*arXiv:astro-ph/0305542* (2003).

[115] WARP Collab., P. Benetti et al., *arXiv:astro-ph/0701286* (2007).

[116]

[117] See *http://hepwww.rl.ac.uk/UKDMC/project/project.html*.

[118] See *http://neutrino.ethz.ch/ArDM/*.

[119] See *http://warp.lngs.infn.it/*.

[120] See *http://xenon.astro.columbia.edu/*.

[121] K. Ni and L. Baudis, *arXiv:astro-ph/0611124* (2006).

[122] XENON Collab., J. Angle et al., *arXiv:0706.0039* [astro-ph] (2007).

[123] The Dark Matter Plotter, *http://dmtools.brown.edu/*.

[124] ZEPLIN Collab., G. J. Alner et al., *arXiv:astro-ph/0701858* (2007).

[125] D. D. Dixon, D. H. Hartmann, E. D. Kolaczyk et al., *New Astronomy*. **3**, 539-561 (1998).

[126] L. Bergstrom, J. Edsjo, M. Gustafsson and P. Salati, *Journal of Cosmology and Astroparticle Physics*. **5**,6 (2006).

[127] P. Gondolo et al., http://www.physto.se/∼ edsjo/darksusy.

[128] R. Abbasi, Y. Abdou, M. Ackermann et al., *Physical Review Letters*. **102**, 20, (2009).

[129] S. Desai, Y. Ashie, S. Fukuda et al., *Physical Review D*. **70**, 8 (2004).

[130] S. W. Barwick, J. J. Beatty, C. R. Bower et al., *Nuclear Instruments and Methods in Physics Research A*. **400**, 34-52 (1997).

[131] S. Haino, K. Abe, K. Anraku et al., *Nuclear Instruments and Methods in Physics Research A*. **518**, 167-171 (2004).

[132] O. Adriani, G. C. Barbarino, G. A. Bazilevskaya et al., *Nature*. **458**, 607-609 (2009).

[133] A. A. Abdo, M. Ackermann, M. Ajello et al., *Physical Review Letters*. **102**, 18 (2009).

[134] F. Aharonian, A. G. Akhperjanian, G. Anton et al., *Astronomy and Astrophysics*. **508**, 561-564 (2009).